



1 Biogenic volatile organic compound ambient mixing ratios and emission rates 2 in the Alaskan Arctic tundra

3 H  l  ne Angot¹, Katelyn McErlean¹, Lu Hu², Dylan B. Millet³, Jacques Hueber¹, Kaixin Cui¹, Jacob Moss¹,
4 Catherine Wielgasz², Tyler Milligan¹, Damien Ketcherside², Marion Sydonia Bret-Harte⁴, Detlev Helmig¹

5 ¹Institute of Arctic and Alpine Research, University of Colorado Boulder, Boulder, CO, USA.

6 ²Department of Chemistry and Biochemistry, University of Montana, Missoula, MT, USA.

7 ³Department of Soil, Water, and Climate, University of Minnesota, Minneapolis-Saint Paul, MN, USA.

8 ⁴Institute of Arctic Biology, University of Alaska-Fairbanks, Fairbanks, Alaska, USA.

9

10 Abstract

11 Rapid Arctic warming, a lengthening growing season, and increasing abundance of biogenic volatile
12 organic compounds (BVOC)-emitting shrubs are all anticipated to increase atmospheric BVOCs in the
13 Arctic atmosphere, with implications for atmospheric oxidation processes and climate feedbacks.
14 Quantifying these changes requires an accurate understanding of the underlying processes driving BVOC
15 emissions in the Arctic. While boreal ecosystems have been widely studied, little attention has been paid to
16 Arctic tundra environments. Here, we report terpenoid (isoprene, monoterpenes, and sesquiterpenes)
17 ambient mixing ratios and emission rates from key dominant vegetation species at Toolik Field Station
18 (TFS; 68°38'N, 149°36'W) in northern Alaska during two back-to-back field campaigns (summers 2018
19 and 2019) covering the entire growing season. Isoprene ambient mixing ratios observed at TFS fell within
20 the range of values reported in the Eurasian taiga (0-500 pptv), while monoterpene and sesquiterpene
21 ambient mixing ratios were respectively close to and below the instrumental quantification limit (~2 pptv).
22 We further quantified the temperature dependence of isoprene emissions from local vegetation including
23 *Salix* spp. (a known isoprene emitter), and compared the results to predictions from the Model of Emissions
24 of Gases and Aerosols from Nature version 2.1 (MEGAN2.1). Our observations suggest a 180-215%
25 emission increase in response to a 3-4°C warming. The MEGAN2.1 temperature algorithm exhibits a close
26 fit with observations for enclosure temperatures below 30°C. Above 30°C, MEGAN2.1 predicts an isoprene
27 emission plateau that is not observed in the enclosure flux measurements at TFS. More studies are needed
28 to better constrain the warming response of isoprene and other BVOCs for a wide range of Arctic species.



29 **1. Introduction**

30 As a major source of reactive carbon to the atmosphere, biogenic volatile organic compounds
31 (BVOCs) emitted from vegetation play a significant role in global carbon and oxidation cycles
32 (Fehsenfeld et al., 1992). Global emission estimates of BVOCs are in the range of 700-1100 TgC
33 per year, ~70-80% of which corresponds to terpenoid species: isoprene, monoterpenes (MT), and
34 sesquiterpenes (SQT) (Guenther et al., 1995, 2006; Sindelarova et al., 2014). Despite their
35 relatively short atmospheric lifetimes (1 hour to 1 day for terpenoids), BVOCs affect climate
36 through their effects on the hydroxyl radical (OH, which dictates the lifetime of atmospheric
37 methane), tropospheric ozone (O₃, a key greenhouse gas), and aerosols (which influence radiative
38 scattering) (Arneth et al., 2010; Fuentes et al., 2000; Peñuelas and Staudt, 2010). The oxidation of
39 those BVOCs also drives the formation of secondary organic aerosols (SOA) through both gas-
40 and aqueous-phase mechanisms (Carlton et al., 2009; Lim et al., 2005). The potential for increased
41 SOA formation, expected to result in climate cooling (Kulmala et al., 2004), complicates the
42 climate feedbacks of BVOC emissions (Tsigaridis and Kanakidou, 2007; Unger, 2014).

43 Global models of BVOC emissions assume minimal emissions from the Arctic due to low leaf
44 area index and relatively cold temperatures (Guenther et al., 2006; Sindelarova et al., 2014).
45 However, this assumption relies on few observations and has been increasingly challenged by field
46 data (Tang et al., 2016). Recent measurements have revealed significant BVOC emissions from
47 Arctic tundra and vegetation, including *Sphagnum* mosses, wetland sedges, and dwarf shrubs
48 (Ekberg et al., 2009, 2011; Faubert et al., 2010; Holst et al., 2010; Lindfors et al., 2000; Potosnak
49 et al., 2013; Rinnan et al., 2011; Schollert et al., 2014; Tiiva et al., 2008). These results are of
50 importance because BVOC emissions are expected to increase in the Arctic due to climate
51 warming and associated vegetation and land cover change (Faubert et al., 2010; Potosnak et al.,
52 2013; Rinnan et al., 2011; Tiiva et al., 2008). Long-term field warming studies have shown strong
53 increases in BVOC emissions from shrub heath (Michelsen et al., 2012; Tiiva et al., 2008).
54 Furthermore, the temperature dependence of Arctic BVOC fluxes appears to be significantly
55 greater than for tropical and subtropical ecosystems (Holst et al., 2010; Rinnan et al., 2014), with
56 up to 2-fold increases in MT emissions and 5-fold increases in SQT emissions by subarctic heath
57 for a 2°C warming (Valolahti et al., 2015). Similarly, Kramshøj et al. (2016) and Lindwall et al.
58 (2016) examined the response of BVOC emissions to an experimental 3-4°C warming and reported



59 a 260-280% increase in total emissions. Together, the above results emphasize the strong
60 temperature sensitivity of BVOC emissions from Arctic ecosystems.

61 Changing BVOC emissions in the Arctic due to climate and land cover shifts can thus be expected
62 to perturb to the overall oxidative chemistry of the region, and to further affect climate through
63 various feedback mechanisms. Quantifying these changes requires an accurate understanding of
64 the underlying processes driving BVOC emissions in the Arctic. While BVOC ambient mixing
65 ratios and emission rates have been studied in boreal ecosystems, less attention has been paid to
66 Arctic tundra environments (Lindwall et al., 2015). Here, we report BVOC ambient mixing ratios
67 and emission rates at Toolik Field Station (TFS) in the Alaskan Arctic. This study builds on the
68 previous isoprene study at TFS by Potosnak et al. (2013), while also providing a major step forward
69 from that work. In particular, we present the first continuous summertime record of ambient
70 BVOCs (including isoprene and MT) and their first-generation oxidation products in the Arctic
71 tundra environment. We further compare the observed temperature dependence of isoprene
72 emissions with predictions from the Model of Emissions of Gases and Aerosols from Nature
73 version 2.1 (MEGAN2.1), a widely used modeling framework for estimating ecosystem-
74 atmosphere BVOC fluxes (Guenther et al., 2012). Due to increasing shrub prevalence across
75 northern Alaska (Berner et al., 2018; Tape et al., 2006), as well as the Eurasian (Macias-Fauria et
76 al., 2012) and Russian Arctic (Forbes et al., 2010), the results of this study have significance to
77 tundra ecosystems across a vast region of the Arctic.

78 2. Material and Methods

79 2.1 Study site

80 This study was carried out at TFS, a Long-Term Ecological Research (LTER) site located in the
81 tundra on the north flanks of the Brooks Range in northern Alaska (68°38'N, 149°36'W; see
82 Fig.1). Vegetation speciation and dynamics, and their changes over time, have been well
83 documented at the site. *Betula* (birch) and *Salix* (willow) are the most common deciduous shrubs
84 (Kade et al., 2012). Common plant species include *Betula nana* (dwarf birch), a major player in
85 ongoing Arctic greening (Holleesen et al., 2015; Sistla et al., 2013), *Rhododendron tomentosum*
86 (formerly *Ledum palustre*; Labrador tea); *Vaccinium vitis-idaea* (lowbush cranberry), *Eriophorum*
87 *vaginatum* (cotton grass), *Sphagnum angustifolium* (peat moss), *Alectoria ochroleuca* (witches
88 hair lichen), and many other perennial species of *Carex*, mosses, and lichens. Vegetation cover at



89 this site is classified as tussock tundra (see Fig.1), which is the most common vegetation type in
90 the northern foothills of the Brooks Range (Elmendorf et al., 2012; Kade et al., 2012; Shaver and
91 Chapin, 1991; Survey, 2012; Walker et al., 1994).

92 Emission measurements and atmospheric sampling were conducted from a weatherproof
93 instrument shelter located ~350 m to the west of TFS (see Fig.S.I.1). Winds at TFS are
94 predominantly from the southerly and northerly sectors (Toolik Field Station Environmental Data
95 Center, 2019), minimizing any influence from camp emissions at the site. Two field campaigns
96 were carried out: the first from mid-July to mid-August 2018, and the second from mid-May to
97 the end of June 2019. These two back-to-back campaigns cover the entire growing season (Sullivan
98 et al., 2007).

99 **2.2 Ambient online measurements of BVOCs and their oxidation products**

100 2.2.1 Gas chromatography and mass spectrometry with flame ionization detector 101 (GC-MS/FID)

102 An automated GC-MS/FID system was deployed for continuous measurements of atmospheric
103 BVOCs at ~2-hour time resolution during the 2018 and 2019 field campaigns. In addition, the
104 system was operated remotely following the 2018 campaign (through September 15th) to collect
105 background values at the beginning of autumn. Air was pulled continuously from an inlet on a 4
106 m meteorological tower located approximately 30 m from the instrument shelter (Van Dam et al.,
107 2013). Air passed through a sodium thiosulfate-coated O₃ scrubber for selective O₃ removal – to
108 prevent sampling losses and artifacts for reactive BVOCs (Helmig, 1997; Pollmann et al., 2005) –
109 and through a moisture trap to dry the air to a dew point of -30°C. Analytes were concentrated on
110 a Peltier-cooled (-40°C) multistage adsorbent trap. Analysis was accomplished by thermal
111 desorption and injection for cryogen free GC using a DB-1 column (60 m × 320 μm × 5 μm) and
112 helium as carrier gas. The oven temperature was set to 40°C for 6 minutes, then increased to 260°C
113 at 20°C/min, and held isothermally at 260°C for 13 minutes. The column flow was split between
114 an FID and a MS for simultaneous quantification and identification. Blanks and calibration
115 standards were regularly injected from a manifold. Isoprene (*m/z* 67 and 68), methacrolein
116 (MACR) and methylvinylketone (MVK) (*m/z* 41, 55, and 70), MT (*m/z* 68, 93, 121, and 136), and
117 SQT (*m/z* 204, 91, 93, 119, and 69) were identified and quantified using the MS in selected ion-
118 monitoring mode (SIM). The response to isoprene was calibrated using a primary gas standard



119 supplied by the National Physical Laboratory (NPL), certified as containing 4.01 ± 0.09 ppb of
120 isoprene in a nitrogen matrix. The analytical uncertainty for isoprene was estimated at 16 % based
121 on the certified uncertainty of the standard and on the repeatability of standard analysis throughout
122 the campaigns. Instrument responses for MACR, MVK, α -pinene, and acetonitrile were calibrated
123 with multi-component standards containing 1007 ppb MACR, 971 ppb MVK, 967 ppb α -pinene,
124 and 1016 ppb acetonitrile (Apel-Riemer Environmental Inc., Miami, FL, USA) dynamically
125 diluted into a stream of ultra-zero grade air to ~ 3 ppb. Quantification of other terpenoid compounds
126 was based on GC peak area (FID response) plus relative response factors using the effective carbon
127 number concept (Faiola et al., 2012; Scanlon and Willis, 1985). The limit of quantification (LOQ)
128 was ~ 2 pptv (pmol/mol by volume). In order to monitor and correct for long-term trends in the
129 detection system, including detector drift and decreasing performance of the adsorbent trap, we
130 used peak areas for long-lived chlorofluorocarbons (CFCs) that were monitored in the air samples
131 together with the BVOCs as an internal reference standard. The atmospheric trace gases CCl_3F
132 (CFC-11) and $\text{CCl}_2\text{FCCl}_2\text{F}_2$ (CFC-113) are ideal in this regard because they are ubiquitous in the
133 atmosphere and exhibit little spatial and temporal variability (Karbiwnyk et al., 2003; Wang et al.,
134 2000).

135 2.2.2 Proton-Transfer-Reaction Time-of-Flight Mass-Spectrometry (PTR-ToF-MS)

136 During the summer 2019 campaign, isoprene mixing ratios in ambient air were also measured by
137 PTR-ToF-MS (model 4000, Ionicon Analytik GmbH, Innsbruck, Austria). The sample inlet was
138 located on the 4 m meteorological tower, right next to the GC-MS/FID inlet. In brief, ambient air
139 was continuously pulled through the PTR-ToF-MS drift-tube, where VOCs with proton affinities
140 higher than that of water (>165.2 kcal/mol) were ionized via proton-transfer reaction with primary
141 H_3O^+ ions, then subsequently separated and detected by a time-of-flight mass spectrometer (with
142 a mass resolving power up to 4000). At TFS, the PTR-ToF-MS measured ions from 17–400 m/z
143 every 2 minutes. Ambient air was drawn to the instrument at 10–15 L/min via ~ 30 m of 1/4" O.D.
144 PFA tubing maintained at $\sim 55^\circ\text{C}$, and then subsampled by the instrument through ~ 100 cm of
145 1/16" O.D. PEEK tubing maintained at 60°C . The residence time from the inlet on the 4 m
146 meteorological tower to the drift-tube was less than 5 seconds. Instrument backgrounds were
147 quantified approximately every 5 hours for 20 minutes during the campaign by measuring VOC-
148 free air generated by passing ambient air through a heated catalytic converter (375°C , platinum



149 bead, 1 % wt. Pt, Sigma Aldrich). Calibrations were typically performed every 4 days via dynamic
150 dilution of certified gas standard mixtures containing 25 distinct VOCs including isoprene (Apel-
151 Riemer Environmental Inc., Miami, FL, USA). Here, we report isoprene mixing ratios to inter-
152 compare with GC-MS measurements; other species will be reported in future work. The
153 measurement uncertainty for isoprene is ~25%, which includes uncertainties in the gas standards,
154 calibration method, and data processing.

155 2.2.3 Instrument inter-comparison

156 Figure S.I.2 shows a comparison of the GC-MS and PTR-ToF-MS isoprene mixing ratios in
157 ambient air. With a correlation coefficient of 0.93 and a linear regression slope of 0.7-1.0, the two
158 measurements agreed within their combined measurement uncertainties, in line with earlier inter-
159 comparison studies (e.g., Dunne et al., 2018; de Gouw et al., 2003). Similarly, we found a
160 correlation coefficient of 0.96 between GC-MS and PTR-ToF-MS MVK+MACR mixing ratios
161 (not shown). The good agreement between these two independent techniques gives us confidence
162 that the ambient air results presented here are robust.

163 2.3 Ambient air vertical profiles

164 Vertical isoprene mixing ratio profiles were obtained using a 12-foot diameter SkyDoc tethered
165 balloon. A total of eight vertical profiles were performed at ~3-hour intervals between 12:30 pm
166 Alaska Standard Time (AST) on June 15, 2019 and 11:00 am AST on June 16, 2019. Sampling
167 packages were connected to the tether line such that resulting sampling heights were ~30, ~100,
168 ~170, and ~240 m above ground level. One identical sampling package was deployed at the
169 surface. Each sampling package contained an adsorbent cartridge for sample collection (see below)
170 connected to a downstream battery-powered SKC pocket pump controlled using a mechanical
171 relay, a programmable Arduino, and a real-time Clock. Once the balloon reached its apex (~ 250-
172 300 m a.g.l.), the five pumps were activated simultaneously and samples collected for 30 minutes.
173 At the end of the 30-min sampling period, the balloon was brought back down. The adsorbent
174 cartridges were prepared in house using glass tubing (89 mm long × 6.4 mm outer diameter, 4.8
175 mm inner diameter), and loaded with Tenax-GR and Carboxen 1016 adsorbents (270 mg of each),
176 following established practice (Ortega and Helmig, 2008 and references therein). An inlet ozone
177 scrubber was installed on each cartridge to prevent BVOC sampling losses. Field blanks were
178 collected by opening a cartridge (with no pumped airflow) during each balloon flight. Following



179 collection, samples were stored in the dark at $\sim 4^{\circ}\text{C}$ until chemical analysis. Samples were analyzed
180 at the University of Colorado Boulder following the method described in S.I. Section 1. Our
181 previous inter-comparison of this cartridge-GC-MS/FID method with independent and concurrent
182 PTR-MS observations showed that the two measurements agree to within their combined
183 uncertainties at $\sim 25\%$ (Hu et al., 2015). Meteorological conditions were monitored and recorded
184 during each balloon flight with a radiosonde (Met1, Grant Pass, OR, USA) attached to the tethered
185 line just below the balloon.

186 **2.4 BVOC emission rates**

187 2.4.1 Dynamic enclosure measurements

188 We used dynamic enclosure systems operated at low residence time to quantify vegetative BVOC
189 emissions following the procedure described by Ortega et al. (2008) and Ortega and Helmig
190 (2008). Two types of enclosures were used: branch and surface chambers. For branch enclosures,
191 a Tedlar® bag (Jensen Inert Products, Coral Springs, FL) was sealed around the trunk side of a
192 branch. For surface enclosures, the bag was placed around a circular Teflon® base (25 cm wide \times
193 16 cm height; see Fig. 2). For both branch and surface enclosures, the bag was connected to a
194 purge-air line and a sampling line, and positioned around the vegetation minimizing contact with
195 foliage. While purging the enclosure (see Section 2.4.3), the vegetation was allowed to acclimate
196 for 24 hours before BVOC sampling began. Samples were collected from the enclosure air,
197 concentrated onto solid-adsorbent cartridges (see Section 2.3) with an automated sampler, and
198 analyzed in-laboratory at the University of Colorado Boulder following the campaign (see S.I.
199 Section 1). Temperature and relative humidity were recorded inside and outside the enclosure (see
200 Fig. 2; S-THB-M002 sensors, Onset HOBO, Bourne, MA, USA) with a data logger (H21-USB,
201 Onset HOBO, Bourne, MA, USA). Additionally, photosynthetically active radiation (400-700 nm;
202 S-LIA-M003, Onset HOBO, Bourne, MA, USA) was measured inside the enclosure. Once
203 installed, enclosures were operated for 2-10 days. The tundra vegetation around TFS is
204 heterogeneous but most dominant species were sampled. Table 1 presents the median relative
205 percent cover of plant species in LTER experimental control plots at TFS (Gough, 2019) and
206 indicates whether plant species were present in surface or bag enclosures. The complete list of
207 species sampled and pictures of the enclosures are available in Figures S.I.3-S.I.15; the two
208 sampling sectors are highlighted in Fig.S.I.1. Surface enclosures were divided into three vegetation



209 types: *Salix* spp. (high isoprene emitter), *Betula* spp. (e.g., *Betula nana* dominance), and
210 miscellaneous (mix of different species, including lichens and mosses).

211 2.4.2 Emission rates

212 The emission rate (ER in $\mu\text{gC}/\text{m}^2/\text{h}$) for surface enclosures was calculated as follows:

$$213 \quad ER_{\text{surface}} = \frac{(C_{\text{out}} - C_{\text{in}})Q}{S}, \quad (1)$$

214 where C_{in} and C_{out} are the inlet and outlet analyte concentrations (in $\mu\text{gC}/\text{L}$), Q is the purge air
215 flow rate (in L/h), and S the surface area of the enclosure (in m^2).

216 The ER for branch enclosures (in $\mu\text{gC}/\text{g}/\text{h}$) was calculated as follows:

$$217 \quad ER_{\text{branch}} = \frac{(C_{\text{out}} - C_{\text{in}})Q}{m_{\text{dry}}}, \quad (2)$$

218 where m_{dry} is the dried mass (in g) of leaves enclosed, determined by drying the leaves – harvested
219 after the experiment – at 60-70°C until a consistent weight was achieved (Ortega and Helmig,
220 2008).

221 2.4.3 Enclosure purge air

222 Purge air was provided by an upstream high-capacity oil-free pump providing positive pressure to
223 the enclosure, and equipped with an in-line O_3 scrubber to avoid loss of reactive BVOCs from
224 reaction with O_3 in the enclosure air and during sampling (Helmig, 1997; Pollmann et al., 2005).
225 The purge flow was set to 25 L/min and regularly checked using a volumetric flow meter (Mesa
226 Labs Bios DryCal Defender, Butler, NJ, USA). Excess air escaped from the open end (tied around
227 the Teflon® base) while the sample air flow was pulled into the sampling line (see below).

228 2.4.4 Sample collection

229 A continuous airflow of 400-500 mL/min was drawn from the enclosure through the sampling line.
230 A fraction of this flow was periodically collected at 265-275 mL/min on adsorbent cartridges (see
231 Section 2.3) using a 10-cartridge autosampler (Helmig et al., 2004). During sampling, cartridges
232 were kept at 40°C, *i.e.*, above ambient temperature, to prevent water accumulation on the adsorbent
233 bed (Karbiwnyk et al., 2002). Samples were periodically collected in series to verify lack of analyte
234 breakthrough. Time-integrated samples were collected for 120 min every 2 hours to establish



235 diurnal cycles of BVOC emission. Upon collection, samples were stored in the dark at $\sim 4^{\circ}\text{C}$ until
236 chemical analysis back at the University of Colorado Boulder.

237 2.4.5 Internal standards

238 In order to identify potential BVOC losses during transport, storage, and chemical analysis, 255
239 of the employed cartridges were pre-loaded with a four-compound standard mixture prior to the
240 field campaigns. These internal standard compounds (toluene, 1, 2, 3-trimethylbenzene, 1, 2, 3, 4-
241 tetrahydronaphtalene, and 1, 3, 5-triisopropylbenzene) were carefully chosen to span a wide range
242 of volatility ($\text{C}_7\text{-C}_{15}$) and to not interfere (*i.e.*, coelute) with targeted BVOCs. The recovery of these
243 four compounds was assessed at the end of the campaign, following the analytical procedure
244 described in S.I. Section 1. Recovery rates were $101.8 \pm 13.5\%$ (toluene), $95.2 \pm 20.1\%$ (1,2,3-
245 trimethylbenzene), $95.6 \pm 26.6\%$ (1,2,3,4-tetrahydronaphtalene), and $100.9 \pm 18.7\%$ (1,3,5-
246 triisopropylbenzene). These results indicate that, overall, BVOC losses during transport, storage,
247 and chemical analysis were negligible. Ortega et al. (2008) previously evaluated systematic losses
248 of analytes to enclosure systems similar to those used here. The same four-component standard
249 was introduced into the purge air flow of the enclosures to quantify losses as a function of
250 volatility. That work found median losses of MT and SQT on the order of 20-30%. The emission
251 rates presented here are therefore possibly biased low by a similar amount.

252 2.5 Peak fitting algorithm

253 The analysis of ambient air and enclosure chromatograms was performed using the TERN
254 (Thermal desorption aerosol GC ExploreR and iNtegration package) peak fitting tool implemented
255 in Igor Pro and available online at <https://sites.google.com/site/terninigor/> (Isaacman-VanWertz et
256 al., 2017).

257 2.6 Ancillary parameters

258 *Meteorological parameters.* A suite of meteorological instruments was deployed on the 4 m tower.
259 Wind speed and direction were measured at ~ 4 m above ground level with a Met One 034B-L
260 sensor. As described by Van Dam et al. (2013), temperature was measured at three different heights
261 using RTD temperature probes (model 41342, R.M. Young Company, Traverse City, MI) housed
262 in aspirated radiation shields (model 43502, R.M. Young Company, Traverse City, MI). Regular
263 same-height inter-comparisons were conducted to test for instrumental offsets. Incoming and



264 reflected solar radiation were recorded with LI200X pyranometers (Campbell Scientific
265 Instruments).

266 In addition, historical (1988-2019) meteorological data recorded by TFS Environmental Data
267 Center are available at: https://toolik.alaska.edu/edc/abiotic_monitoring/data_query.php

268 *Particle measurements.* A Met One Instruments Model 212-2 8-channel (0.3 to 10 μm) particle
269 profiler was operated continuously on the roof of the weatherproof instrument shelter. This
270 instrument uses a laser-diode based optical sensor and light scatter technology to detect, size, and
271 count particles (<http://mail.metone.com/particulate-Aero212.htm>).

272 *Nitrogen oxides.* Nitrogen oxides (NO_x) were measured with a custom-built, high sensitivity (~ 5
273 pptv detection limit) single-channel chemiluminescence analyzer (Fontijn et al., 1970). The
274 instrument monitors nitric oxide (NO) and nitrogen dioxide (NO_2) in ambient air using a photolytic
275 converter. Automated switching valves alternated between NO and NO_2 mode every 30 minutes.
276 Calibration was accomplished by dynamic dilution of a 1.5 ppm compressed NO gas standard
277 (Scott-Marrin, Riverside, CA, USA).

278 **2.7 Theoretical response of isoprene emissions to temperature in MEGAN2.1**

279 We applied our isoprene emission measurements to evaluate the temperature response algorithms
280 embedded in MEGAN2.1 (Guenther et al., 2012). Theoretical isoprene emission rates (F_T) were
281 calculated for TFS as:

$$282 \quad F_T = C_{CE} \gamma_T \sum_j \kappa_j \varepsilon_j \quad (3)$$

283 where C_{CE} is the canopy environment coefficient (assigned a value that results in $\gamma_T = 1$ under
284 standard conditions), and ε_j is the emission factor under standard conditions for vegetation type j
285 with fractional grid box areal coverage κ_j . We used $\sum_j \kappa_j \varepsilon_j = 2766 \mu\text{g}/\text{m}^2/\text{h}$ at TFS based on the
286 high resolution (1 km) global emission factor input file available at
287 <https://bai.ess.uci.edu/megan/data-and-code/megan21>. The temperature activity factor (γ_T) was
288 calculated as:

$$289 \quad \gamma_T = E_{opt} \times \frac{200 e^{95x}}{200 - 95 \times (1 - e^{200x})} \quad (4)$$

290 with



291
$$x = \frac{\frac{1}{T_{opt}} - \frac{1}{T}}{0.00831} \quad (5)$$

292
$$E_{opt} = 2 \times e^{0.08(T_{10} - 297)} \quad (6)$$

293
$$T_{opt} = 313 + 0.6(T_{10} - 297), \quad (7)$$

294 where T is the enclosure ambient air temperature and T_{10} the average enclosure air temperature
295 over the past 10 days.

296 3. Results and Discussion

297 3.1 Ambient air mixing ratios

298 3.1.1 Isoprene and oxidation products

299 Figure 3 (top panels) shows the time-series of isoprene mixing ratios in ambient air recorded over
300 the course of this study at TFS with the GC system. Mixing ratios were highly variable and ranged
301 from below the quantification limit to 505 pptv (mean of 36.1 pptv). The PTR-ToF-MS gave
302 similar results (see Fig.S.I.16a). These mixing ratios fall within the range of values reported in the
303 Eurasian taiga (e.g., Hakola et al., 2000, 2003; Lappalainen et al., 2009). For example, Hakola et
304 al. (2003) reported a maximum monthly mean mixing ratio of 98 pptv (in July) in Central Finland
305 while Hakola et al. (2000) observed mixing ratios ranging from a few pptv to ~600 pptv in Eastern
306 Finland. In general, however, BVOC emissions in the Eurasian taiga are relatively low compared
307 to forest ecosystems in warmer climates and are dominated by monoterpenes (Rinne et al., 2009).

308 Isoprene mixing ratios peaked on August 1, 2018 around 4 pm and on June 20, 2019 around 10
309 pm, respectively. These two peaks occurred 3-5 hours after the daily maximum ambient
310 temperature was reached (17.8°C in 2018 and 21.8°C in 2019 – see Fig. 3). The isoprene peak on
311 June 20, 2019 was concomitant with enhanced acetonitrile mixing ratios and particle counts (see
312 Fig. 4), reflecting unusually hazy conditions that day at TFS. We attribute the particle and
313 acetonitrile enhancements to intense wildfires occurring across the Arctic Circle at that time – most
314 of them in southern Alaska and Siberia (Earth Observatory, 2019). Acetonitrile increased by a
315 factor of 4 during this event, compared to a factor of 21 increase for isoprene. The higher emission
316 factor for acetonitrile vs. isoprene from biomass burning in boreal forests (Akagi et al., 2011) and
317 the relatively short lifetime of isoprene (Atkinson, 2000) indicate that the observed isoprene
318 enhancement was due to fresh local biogenic emissions rather than transported wildfire emissions.



319 Over the course of this study, we recorded MACR and MVK mixing ratios respectively ranging
320 from below the quantification limit to 95 pptv (12.4 ± 16.1 pptv; mean \pm standard deviation) and
321 from below the quantification limit to 450 pptv (43.1 ± 66.7 pptv; see Fig. 3, top panels). The PTR-
322 ToF-MS gave similar results (see Fig.S.I.16b). Median NO and NO₂ mixing ratios of 21 and 74
323 pptv, respectively, during the 2019 campaign (not shown) suggest a low-NO_x environment, in line
324 with previous studies at several Arctic locations (Bakwin et al., 1992; Honrath and Jaffe, 1992).
325 Under such conditions, MACR and MVK mixing ratios should be used as upper estimates as it has
326 been noted that some low-NO_x isoprene oxidation products (isoprene hydroxyhydroperoxides) can
327 undergo rearrangement in GC and PTR-MS instruments and be misidentified as MACR and MVK
328 (Rivera-Rios et al., 2014). We found a high correlation between MACR and MVK ($R^2 = 0.95$, $p <$
329 0.01) and between these two compounds and isoprene ($R^2 \sim 0.80$, $p < 0.01$). Increases of MACR
330 and MVK mixing ratios above the background were mostly concomitant with isoprene increases,
331 suggesting that atmospheric or within-plant oxidation of isoprene was their main source
332 (Biesenthal et al., 1997; Hakola et al., 2003; Jardine et al., 2012). The mean ratio of MVK to
333 MACR was 2.7, within the range reported by earlier studies (e.g., Apel et al., 2002; Biesenthal and
334 Shepson, 1997; Hakola et al., 2003; Helmig et al., 1998), and no clear diurnal cycle in the ratio
335 was found.

336 3.1.2 Isoprene vertical profiles

337 Figure 5 shows vertical profiles (0 to ~ 250 m a.g.l.) of isoprene mixing ratios derived from the 30-
338 min tethered balloon samples collected on June 15 and 16, 2019 (see Section 2.3). Temperature
339 profiles (see Fig.S.I.17) indicate that most of the flights were performed in a convective boundary
340 layer (Holton and Hakim, 2013). A nocturnal boundary layer was, however, observed in the first
341 ~ 50 m from ~ 2 am to $\sim 4:30$ am (see Fig.S.I.17e-f) – with temperature increasing with elevation.

342 Except during the last flight, isoprene mixing ratios were in the range of background levels (~ 0 -
343 50 pptv) reported with the GC-MS (see Section 3.1.1). Samples collected on June 16, 2019 from
344 4 to 4:30 am show decreasing isoprene mixing ratios with increasing elevation, suggesting higher
345 levels (25 - 50 pptv) in the nocturnal boundary layer than above. Samples collected from 10-10:30
346 am on June 16 (*i.e.*, during the last flight) showed a pronounced gradient, with 200 pptv at ground
347 level and decreasing mixing ratios with elevation. This maximum at ground-level is consistent
348 with a surface source (Helmig et al., 1998) and can likely be attributed to a temperature-driven



349 increase of isoprene emissions by the surrounding vegetation. Indeed, the ambient temperature at
350 ground-level was higher during that flight than during the previous ones (see Fig.S.I.17h).
351 Interestingly, the GC-MS and the PTR-ToF-MS did not capture this 200 pptv maximum (see Fig.
352 3 and Fig.S.I.16), which may be because the balloon flights were performed at a different location
353 (near sampling sector B, see Fig.S.I.1) surrounded by a higher fraction of isoprene-emitting shrubs
354 (willow).

355 3.1.3 Monoterpenes and Sesquiterpenes

356 MT mixing ratios ranged from 3 to 537 pptv (14 ± 18 pptv; median \pm standard deviation) during
357 the 2019 campaign according to the PTR-ToF-MS measurements. Using the GC-MS/FID, we were
358 able to detect and quantify the following MT in ambient air: α -pinene, camphene, sabinene, p-
359 cymene, and limonene. Mean mixing ratios are reported in Table 2 (for values lower than the LOQ,
360 mixing ratios equal to half of the LOQ are used). These compounds have been previously identified
361 as emissions of the widespread circumpolar dwarf birch *Betula nana* (Li et al., 2019; Vedel-
362 Petersen et al., 2015) and other high Arctic vegetation (Schollert et al., 2014). The quantification
363 frequency of camphene, sabinene, p-cymene, and limonene was low (see Table 2) and MT mixing
364 ratios in ambient air were dominated by α -pinene. Several prior studies performed at boreal sites
365 have similarly identified α -pinene as the most abundant monoterpene throughout the growing
366 season (e.g., Hakola et al., 2000; Lindfors et al., 2000; Spirig et al., 2004; Tarvainen et al., 2007).
367 We did not detect any sesquiterpene in ambient air above the 2 pptv instrumental LOQ.

368 Overall, isoprene and α -pinene dominated the ambient air BVOC profile at TFS, respectively
369 constituting ~72% and ~24% of total BVOCs quantified in ambient air (on a mixing-ratio basis).

370 3.2 Emission rates

371 3.2.1 Branch enclosures

372 A branch enclosure experiment was performed from July 27 to August 2, 2018 on *Salix glauca* to
373 investigate BVOC emission rates per dry weight plant biomass (see Fig.S.I.5). Isoprene emission
374 rates ranged from <0.01 to 11 $\mu\text{gC/g/h}$, in line with results reported for the same species at
375 Kobbefjord, Greenland (0.8 to 12.1 $\mu\text{gC/g/h}$) by Vedel-Petersen et al. (2015) and Kramshøj et al.
376 (2016; Supplementary Table 5). The quantified MTs had emissions averaging two orders of
377 magnitude lower than those of isoprene (0.01 vs 1 $\mu\text{gC/g/h}$). Emission rates for the sum of α -



378 pinene, β -pinene, limonene, camphene, and 1,8-cineole ranged from <0.01 to $0.06 \mu\text{gC/g/h}$. These
379 results are again in good agreement with those reported for the same species at Kobbefjord (~ 0.01
380 $\mu\text{gC/g/h}$) by Kramshøj et al. (2016; Supplementary Table 5).

381 3.2.2 Surface emission rates

382 The isoprene surface emission rate, as inferred from surface enclosures, was highly variable and
383 ranged from 0.2 to $\sim 2250 \mu\text{gC/m}^2/\text{h}$ (see Fig. 6). The $2250 \mu\text{gC/m}^2/\text{h}$ maximum, reached on June
384 26, 2019, is higher than maximum values reported at TFS by Potosnak et al. (2013) (1200
385 $\mu\text{gC/m}^2/\text{h}$) and in a high-latitude (58°N) *Salix* plantation by Olofsson et al. (2005) ($730 \mu\text{gC/m}^2/\text{h}$).
386 It should be noted that these experiments were likely performed at different ambient temperatures.
387 We further investigate the temperature dependency of isoprene emissions in Section 3.3. Elevated
388 surface emission rates (*i.e.*, $> 500 \mu\text{gC/m}^2/\text{h}$) were all observed while sampling enclosures
389 dominated by *Salix* spp.. At TFS, the overall mean isoprene emission rate amounted to 85
390 $\mu\text{gC/m}^2/\text{h}$ while the daytime (10 am-8 pm) and midday (11 am-2 pm) means were 140 and 213
391 $\mu\text{gC/m}^2/\text{h}$, respectively. To put this in perspective, isoprene surface emission rates were much
392 lower than for mid-latitude or tropical forests. For example, average midday fluxes of 3000
393 $\mu\text{gC/m}^2/\text{h}$ were reported in a northern hardwood forest in Michigan (Pressley et al., 2005), while
394 several reports of isoprene emissions from tropical ecosystems give daily estimates of 2500 - 3000
395 $\mu\text{gC/m}^2/\text{h}$ (Helmig et al., 1998; Karl et al., 2004; Rinne et al., 2002).

396 Figure 7 shows the measured surface emission rates for α -pinene, β -pinene, limonene, and 1,8-
397 cineole. While *p*-cymene, sabinene, 3-carene, and isocaryophyllene (SQT) were detected in some
398 of the surface enclosure samples, we focus the discussion on the most frequently quantified
399 compounds. Regardless of the species, emission rates remained on average below $1 \mu\text{gC/m}^2/\text{h}$ over
400 the course of the study (see Table 3). These results are at the low end of emission rates reported
401 for four vegetation types in high Arctic Greenland (Schollert et al., 2014), but in line with results
402 reported at Kobbefjord, Greenland by Kramshøj et al. (2016; Supplementary Table 4).

403 Figures 8a-c show the mean diurnal cycle (over the two campaigns) of isoprene surface emission
404 rates for different vegetation types (see Fig.S.I.3-15 for nomenclature). Regardless of the
405 vegetation type, isoprene emission rates exhibited a significant diurnal cycle with an early
406 afternoon maximum, in line with the mean diurnal cycle of enclosure temperature and PAR. These



407 results are in line with the well-established diurnal variation of BVOC emissions in environments
408 ranging from Mediterranean to boreal forests (e.g., Fares et al., 2013; Liu et al., 2004; Ruuskanen
409 et al., 2005; Zini et al., 2001). Despite the relatively low MT emission rates, a significant diurnal
410 cycle was also observed with peak total MT emissions of $\sim 1 \mu\text{gC}/\text{m}^2/\text{h}$ during early afternoon for
411 both *Salix* spp. and *Betula* spp. (Fig. 8e-f). A summary of emission rates per vegetation type and
412 time of day is given in Table 3. It should be noted that the two field campaigns were carried out
413 during the midnight sun period, which could possibly sustain BVOC emissions during nighttime.
414 As can be seen in Table 3 and Fig. 8, PAR and BVOC emissions significantly decreased at night
415 but were still detectable. These results confirm those obtained by Lindwall et al. (2015) during a
416 24-hour experiment with five different Arctic vegetation communities.

417 The ratio of total MT (given by the sum of α -pinene, β -pinene, limonene, and 1,8-cineole)
418 emissions to isoprene emissions was an order of magnitude higher for *Betula* spp. (0.22) than for
419 *Salix* spp. (0.03). This result, driven by the relatively lower isoprene emissions of *Betula* spp., is
420 in line with earlier studies, suggesting similar emission characteristics for Arctic plants (e.g.,
421 Kramshøj et al., 2016; Vedel-Petersen et al., 2015).

422 **3.3 Response of isoprene emissions to temperature**

423 The Arctic has warmed significantly during the last three decades and temperatures are projected
424 to increase an additional 5-13°C by the end of the century (Overland et al., 2014). Heat wave
425 frequency is also increasing in the terrestrial Arctic (Dobricic et al., 2020). For example, western
426 Siberia experienced an unusually warm May in 2020, with temperatures of 20-25°C (Freedman
427 and Cappucci, 2020). In that context, numerous studies have pointed out the likelihood of increased
428 BVOC emissions due to Arctic warming and associated vegetation and land cover change (Faubert
429 et al., 2010; Potosnak et al., 2013; Rinnan et al., 2011; Tiiva et al., 2008).

430 Over the course of the two field campaigns at TFS, BVOC surface emission rates were measured
431 over a large span of enclosure temperatures (2-41°C). While MT emissions remained low and close
432 to the detection limit thus preventing robust quantification of any emission-temperature
433 relationship, isoprene emissions significantly increased with temperature (Fig.9). Figure 9
434 combines isoprene emission rates from different surface enclosures, with results normalized to
435 account for differing leaf area and species distributions (with *Salix* spp. the dominant emitter).
436 Specifically, we divided all fluxes by the enclosure-specific mean emission at $20 \pm 1^\circ\text{C}$. Emission



437 rates are often standardized to 30°C but we employ 20°C here owing to the colder growth
438 environment at TFS (Ekberg et al., 2009). The isoprene emission-temperature relationship
439 observed at TFS (in blue) is very similar to that reported by Tang et al. (2016) at Abisko (Sweden;
440 in pink) for tundra heath (dominated by evergreen and deciduous dwarf shrubs). Results at TFS
441 and Abisko both point to a high isoprene-temperature response for Arctic ecosystems (Tang et al.,
442 2016). This is further supported by two warming experiments performed in mesic tundra heath
443 (dominated by *Betula nana*, *Empetrum nigrum*, *Empetrum hermaphroditum*, and *Cassiope*
444 *tetragona*) and dry dwarf-shrub tundra (co-dominated by *Empetrum hermaphroditum* and *Salix*
445 *glauca*) in Western Greenland (Kramshøj et al., 2016; Lindwall et al., 2016). Kramshøj et al.
446 (2016) observed a 240% isoprene emission increase with 3°C warming, while Lindwall et al.
447 (2016) reported a 280% increase with 4°C warming. The observationally-derived emission-
448 temperature relationship derived here for TFS reveals a 180-215% emission increase with 3-4°C
449 warming, adding to a growing body of evidence indicating a high isoprene-temperature response
450 in Arctic ecosystems.

451 The MEGAN2.1 modeling framework is commonly used to estimate BVOC fluxes between
452 terrestrial ecosystems and the atmosphere (e.g., Millet et al., 2018). Here, we apply the TFS
453 observations to evaluate the MEGAN2.1 emission-temperature relationship for this Arctic
454 environment. Figure 9 shows that the model temperature algorithm provides a close fit with
455 observations below 30°C, with a 170-240% emission increase for a 3-4°C warming. However, the
456 model predicts a leveling-off of emissions at approximately 30-35°C, whereas our observations
457 reveal no such leveling-off within the 0-40°C enclosure temperature range (Fig. 9). Current models
458 can therefore be expected to strongly underpredict isoprene emissions in this region for
459 temperatures above 30°C.

460 To put the above finding in perspective, the highest air temperature on record at TFS (1988-2019)
461 is 26.5°C, and the mean summertime (June-August) temperature over that period is 9°C. Only 1-
462 23 and 0-4 days per year over that timespan recorded daily maximum temperatures above 20°C
463 and 25°C, respectively. If global greenhouse gas emissions continue to increase, temperatures are
464 expected to rise 6-7°C in northern Alaska by the end of the century (annual average; Markon et
465 al., 2012) while the number of days with temperatures above 25°C could triple (Lader et al., 2017).
466 Based on current climate conditions and this rate of change, the MEGAN2.1 algorithm can still be



467 expected to adequately represent the temperature dependence response of Arctic ecosystems for
468 the near and intermediate-term future.

469 **4. Implications and conclusions**

470 While BVOC ambient concentrations and emission rates have been frequently measured in boreal
471 ecosystems, Arctic tundra environments are scarcely studied. We provide here summertime BVOC
472 ambient air mixing ratios and emission rates at Toolik Field Station, on the north flanks of the
473 Brooks Range in northern Alaska. These data provide a baseline to investigate future changes in
474 the BVOC emission potential of the Arctic tundra environment. Elevated isoprene surface
475 emission rates ($> 500 \mu\text{gC}/\text{m}^2/\text{h}$) were observed for *Salix* spp., a known isoprene emitter. The
476 response to temperature of isoprene emissions in enclosures dominated by *Salix* spp. increased
477 exponentially in the 0-40°C range, likely conferring greater thermal protection for these plants.
478 Our study indicates that the temperature algorithm in MEGAN2.1, a widely used modelling
479 framework for BVOC emissions, provides a good fit with observations in the Arctic tundra for
480 temperatures below 30°C. However, more studies are needed to better constrain the warming
481 response of isoprene and other BVOCs for a wider range of Arctic species.

482 In the context of a widespread increase in shrub abundance (including *Salix* spp.) in the Arctic
483 (Berner et al., 2018; Sturm et al., 2001) due to a longer growing season and enhanced nutrient
484 availability, our results support earlier studies (e.g., Valolahti et al., 2015) suggesting that climate-
485 induced changes in the Arctic vegetation composition will likely significantly affect the BVOC
486 emission potential of the Arctic tundra. As discussed extensively by Peñuelas and Staudt (2010)
487 and Loreto and Schnitzler (2010), emissions of BVOCs might be largely beneficial for plants,
488 conferring them higher protection from abiotic stressors (e.g., heat, air pollution, high irradiance)
489 which are predicted to be more severe in the future. Arctic warming may thus favor BVOC-
490 emitting species even further.

491 **Data availability**

492 Data are available upon request to the corresponding author.

493 **Author contribution**



494 DH, LH, and DBM designed the experiments and acquired funding. HA led the two field
495 campaigns with significant on-site contribution from KM, JH, LH, DBM, KC, JM, CW, TM, and
496 DH. JH designed and built most of the instruments used in this study. CW acquired the PTR-ToF-
497 MS data during the second campaign and DK performed data analysis. MSBH identified the plant
498 species and provided guidance during the field campaigns. KM and HA analyzed the samples in
499 the lab. HA analyzed all the data and prepared the manuscript with contributions from all co-
500 authors.

501 **Competing interests**

502 The authors declare no competing interests.

503 **Acknowledgements**

504 The authors would like to thank CH2MHill Polar Services for logistical support, the Toolik Field
505 Station staff for assistance with the measurements, and Ilann Bourgeois and Georgios Gkatzelis
506 for helpful discussions. The authors also appreciate the help of Anssi Liikanen who offered kind
507 assistance collecting BVOC samples with the tethered balloon and Wade Permar who helped with
508 PTR-ToF-MS measurements. Finally, the authors gratefully acknowledge Claudia Czimczik and
509 Shawn Pedron at the University of California Irvine for letting us use their soil chamber collars.
510 This research was funded by the National Science Foundation grant #1707569. Undergraduate
511 students Katelyn McErlean, Jacob Moss, and Kaixin Cui received financial support from the
512 University of Colorado Boulder's Undergraduate Research Opportunities Program (UROP;
513 reference #5352323, #4422751, and #4332562, respectively).



514 References

- 515 Akagi, S. K., Yokelson, R. J., Wiedinmyer, C., Alvarado, M. J., Reid, J. S., Karl, T., Crounse, J.
516 D. and Wennberg, P. O.: Emission factors for open and domestic biomass burning for use in
517 atmospheric models, *Atmospheric Chem. Phys.*, 11(9), 4039–4072,
518 doi:https://doi.org/10.5194/acp-11-4039-2011, 2011.
- 519 Apel, E. C., Riemer, D. D., Hills, A., Baugh, W., Orlando, J., Faloona, I., Tan, D., Brune, W.,
520 Lamb, B., Westberg, H., Carroll, M. A., Thornberry, T. and Geron, C. D.: Measurement and
521 interpretation of isoprene fluxes and isoprene, methacrolein, and methyl vinyl ketone mixing ratios
522 at the PROPHET site during the 1998 Intensive, *J. Geophys. Res. Atmospheres*, 107(D3), ACH 7-
523 1-ACH 7-15, doi:10.1029/2000JD000225, 2002.
- 524 Arneth, A., Harrison, S. P., Zaehle, S., Tsigaridis, K., Menon, S., Bartlein, P. J., Feichter, J.,
525 Korhola, A., Kulmala, M., O'Donnell, D., Schurgers, G., Sorvari, S. and Vesala, T.: Terrestrial
526 biogeochemical feedbacks in the climate system, *Nat. Geosci.*, 3(8), 525–532,
527 doi:10.1038/ngeo905, 2010.
- 528 Atkinson, R.: Atmospheric chemistry of VOCs and NO_x, *Atmos. Environ.*, 34(12), 2063–2101,
529 doi:10.1016/S1352-2310(99)00460-4, 2000.
- 530 Bakwin, P. S., Wofsy, S. C., Fan, S.-M. and Fitzjarrald, D. R.: Measurements of NO_x and NO_y
531 concentrations and fluxes over Arctic tundra, *J. Geophys. Res. Atmospheres*, 97(D15), 16545–
532 16557, doi:10.1029/91JD00929, 1992.
- 533 Berner, L. T., Jantz, P., Tape, K. D. and Goetz, S. J.: Tundra plant above-ground biomass and
534 shrub dominance mapped across the North Slope of Alaska, *Environ. Res. Lett.*, 13(3), 035002,
535 doi:10.1088/1748-9326/aaa9a, 2018.
- 536 Biesenthal, T. A. and Shepson, P. B.: Observations of anthropogenic inputs of the isoprene
537 oxidation products methyl vinyl ketone and methacrolein to the atmosphere, *Geophys. Res. Lett.*,
538 24(11), 1375–1378, doi:10.1029/97GL01337, 1997.
- 539 Biesenthal, T. A., Wu, Q., Shepson, P. B., Wiebe, H. A., Anlauf, K. G. and Mackay, G. I.: A study
540 of relationships between isoprene, its oxidation products, and ozone, in the Lower Fraser Valley,
541 BC - ScienceDirect, *Atmospheric Environment*, 31(14), 2049–2058, 1997.
- 542 Carlton, A. G., Wiedinmyer, C. and Kroll, J. H.: A review of Secondary Organic Aerosol (SOA)
543 formation from isoprene, *Atmospheric Chem. Phys.*, 9(14), 4987–5005,
544 doi:https://doi.org/10.5194/acp-9-4987-2009, 2009.
- 545 Dobricic, S., Russo, S., Pozzoli, L., Wilson, J. and Vignati, E.: Increasing occurrence of heat waves
546 in the terrestrial Arctic, *Environ. Res. Lett.*, 15(2), 024022, doi:10.1088/1748-9326/ab6398, 2020.
- 547 Dunne, E., Galbally, I. E., Cheng, M., Selleck, P., Molloy, S. B. and Lawson, S. J.: Comparison
548 of VOC measurements made by PTR-MS, adsorbent tubes–GC-FID-MS and DNPH
549 derivatization–HPLC during the Sydney Particle Study, 2012: a contribution to the assessment of



- 550 uncertainty in routine atmospheric VOC measurements, *Atmospheric Meas. Tech.*, 11(1), 141–
551 159, doi:<https://doi.org/10.5194/amt-11-141-2018>, 2018.
- 552 Earth Observatory: Arctic Fires Fill the Skies with Soot, [online] Available from:
553 [https://earthobservatory.nasa.gov/images/145380/arctic-fires-fill-the-skies-with-](https://earthobservatory.nasa.gov/images/145380/arctic-fires-fill-the-skies-with-soot#targetText=In%20June%20and%20July%202019,harmful%20particles%20into%20the%20air.(Accessed%2016%20October%202019),2019)
554 [soot#targetText=In%20June%20and%20July%202019,harmful%20particles%20into%20the%20](https://earthobservatory.nasa.gov/images/145380/arctic-fires-fill-the-skies-with-soot#targetText=In%20June%20and%20July%202019,harmful%20particles%20into%20the%20air.(Accessed%2016%20October%202019),2019)
555 [air. \(Accessed 16 October 2019\)](https://earthobservatory.nasa.gov/images/145380/arctic-fires-fill-the-skies-with-soot#targetText=In%20June%20and%20July%202019,harmful%20particles%20into%20the%20air.(Accessed%2016%20October%202019),2019), 2019.
- 556 Ekberg, A., Arneth, A., Hakola, H., Hayward, S. and Holst, T.: Isoprene emission from wetland
557 sedges, *Biogeosciences*, 6(4), 601–613, doi:10.5194/bg-6-601-2009, 2009.
- 558 Ekberg, A., Arneth, A. and Holst, T.: Isoprene emission from Sphagnum species occupying
559 different growth positions above the water table, *Boreal Environ. Res. Int. Interdiscip. J.*, 16(1),
560 47–59, 2011.
- 561 Elmendorf, S. C., Henry, G. H. R., Hollister, R. D., Björk, R. G., Boulanger-Lapointe, N., Cooper,
562 E. J., Cornelissen, J. H. C., Day, T. A., Dorrepaal, E., Elumeeva, T. G., Gill, M., Gould, W. A.,
563 Harte, J., Hik, D. S., Hofgaard, A., Johnson, D. R., Johnstone, J. F., Jónsdóttir, I. S., Jorgenson, J.
564 C., Klanderud, K., Klein, J. A., Koh, S., Kudo, G., Lara, M., Lévesque, E., Magnússon, B., May,
565 J. L., Mercado-Díaz, J. A., Michelsen, A., Molau, U., Myers-Smith, I. H., Oberbauer, S. F.,
566 Onipchenko, V. G., Rixen, C., Schmidt, N. M., Shaver, G. R., Spasojevic, M. J., Þórhallsdóttir, Þ.
567 E., Tolvanen, A., Troxler, T., Tweedie, C. E., Villareal, S., Wahren, C.-H., Walker, X., Webber,
568 P. J., Welker, J. M. and Wipf, S.: Plot-scale evidence of tundra vegetation change and links to
569 recent summer warming, *Nat. Clim. Change*, 2(6), 453–457, doi:10.1038/nclimate1465, 2012.
- 570 Faiola, C. L., Erickson, M. H., Fricaud, V. L., Jobson, B. T. and VanReken, T. M.
571 (orcid:0000000226454911): Quantification of biogenic volatile organic compounds with a flame
572 ionization detector using the effective carbon number concept, *Atmospheric Meas. Tech. Online*,
573 5(8), doi:10.5194/amt-5-1911-2012, 2012.
- 574 Fares, S., Schnitzhofer, R., Jiang, X., Guenther, A., Hansel, A. and Loreto, F.: Observations of
575 Diurnal to Weekly Variations of Monoterpene-Dominated Fluxes of Volatile Organic Compounds
576 from Mediterranean Forests: Implications for Regional Modeling, *Environ. Sci. Technol.*, 47(19),
577 11073–11082, doi:10.1021/es4022156, 2013.
- 578 Faubert, P., Tiiva, P., Rinnan, Å., Michelsen, A., Holopainen, J. K. and Rinnan, R.: Doubled
579 volatile organic compound emissions from subarctic tundra under simulated climate warming,
580 *New Phytol.*, 187(1), 199–208, doi:10.1111/j.1469-8137.2010.03270.x, 2010.
- 581 Fehsenfeld, F., Calvert, J., Fall, R., Goldan, P., Guenther, A. B., Hewitt, C. N., Lamb, B., Liu, S.,
582 Trainer, M., Westberg, H. and Zimmerman, P.: Emissions of volatile organic compounds from
583 vegetation and the implications for atmospheric chemistry, *Glob. Biogeochem. Cycles*, 6(4), 389–
584 430, doi:10.1029/92GB02125, 1992.
- 585 Fontijn, Arthur., Sabadell, A. J. and Ronco, R. J.: Homogeneous chemiluminescent measurement
586 of nitric oxide with ozone. Implications for continuous selective monitoring of gaseous air
587 pollutants, *Anal. Chem.*, 42(6), 575–579, doi:10.1021/ac60288a034, 1970.



- 588 Forbes, B. C., Fauria, M. M. and Zetterberg, P.: Russian Arctic warming and ‘greening’ are closely
589 tracked by tundra shrub willows, *Glob. Change Biol.*, 16(5), 1542–1554, doi:10.1111/j.1365-
590 2486.2009.02047.x, 2010.
- 591 Freedman, A. and Cappucci, M.: Parts of Siberia are hotter than Washington, with temperatures
592 nearly 40 degrees above average, *Wash. Post*, 22nd May [online] Available from:
593 <https://www.washingtonpost.com/weather/2020/05/22/siberia-heat-wave/> (Accessed 29 May
594 2020), 2020.
- 595 Fuentes, J. D., Lerdau, M., Atkinson, R., Baldocchi, D., Bottenheim, J. W., Ciccioli, P., Lamb, B.,
596 Geron, C., Gu, L., Guenther, A., Sharkey, T. D. and Stockwell, W.: Biogenic Hydrocarbons in the
597 Atmospheric Boundary Layer: A Review, *Bull. Am. Meteorol. Soc.*, 81(7), 1537–1576,
598 doi:10.1175/1520-0477(2000)081<1537:BHITAB>2.3.CO;2, 2000.
- 599 Gough, L.: Relative percent cover of plant species for years 2012-2017 in the Arctic Long-term
600 Ecological Research (ARC-LTER) 1989 moist acidic tundra (MAT89) experimental plots, Toolik
601 Field Station, Alaska., , doi:10.6073/PASTA/F31DEF760DB3F8E6CFEE5FEE07CC693E, 2019.
- 602 de Gouw, J. A., Goldan, P. D., Warneke, C., Kuster, W. C., Roberts, J. M., Marchewka, M.,
603 Bertman, S. B., Pszenny, A. a. P. and Keene, W. C.: Validation of proton transfer reaction-mass
604 spectrometry (PTR-MS) measurements of gas-phase organic compounds in the atmosphere during
605 the New England Air Quality Study (NEAQS) in 2002, *J. Geophys. Res. Atmospheres*, 108(D21),
606 doi:10.1029/2003JD003863, 2003.
- 607 Guenther, A., Hewitt, C. N., Erickson, D., Fall, R., Geron, C., Graedel, T., Harley, P., Klinger, L.,
608 Lerdau, M., Mckay, W. A., Pierce, T., Scholes, B., Steinbrecher, R., Tallamraju, R., Taylor, J. and
609 Zimmerman, P.: A global model of natural volatile organic compound emissions, *J. Geophys. Res.*
610 *Atmospheres*, 100(D5), 8873–8892, doi:10.1029/94JD02950, 1995.
- 611 Guenther, A., Karl, T., Harley, P., Wiedinmyer, C., Palmer, P. I. and Geron, C.: Estimates of global
612 terrestrial isoprene emissions using MEGAN (Model of Emissions of Gases and Aerosols from
613 Nature), *Atmospheric Chem. Phys.*, 6(11), 3181–3210, doi:[https://doi.org/10.5194/acp-6-3181-](https://doi.org/10.5194/acp-6-3181-2006)
614 2006, 2006.
- 615 Guenther, A. B., Jiang, X., Heald, C. L., Sakulyanontvittaya, T., Duhl, T., Emmons, L. K. and
616 Wang, X.: The Model of Emissions of Gases and Aerosols from Nature version 2.1 (MEGAN2.1):
617 an extended and updated framework for modeling biogenic emissions, *Geosci. Model Dev.*, 5(6),
618 1471–1492, doi:<https://doi.org/10.5194/gmd-5-1471-2012>, 2012.
- 619 Hakola, H., Laurila, T., Rinne, J. and Puhto, K.: The ambient concentrations of biogenic
620 hydrocarbons at a northern European, boreal site, *Atmos. Environ.*, 34(29), 4971–4982,
621 doi:10.1016/S1352-2310(00)00192-8, 2000.
- 622 Hakola, H., Tarvainen, V., Laurila, T., Hiltunen, V., Hellén, H. and Keronen, P.: Seasonal variation
623 of VOC concentrations above a boreal coniferous forest, *Atmos. Environ.*, 37(12), 1623–1634,
624 doi:10.1016/S1352-2310(03)00014-1, 2003.



- 625 Helmig, D.: Ozone removal techniques in the sampling of atmospheric volatile organic trace gases,
626 *Atmos. Environ.*, 31(21), 3635–3651, doi:10.1016/S1352-2310(97)00144-1, 1997.
- 627 Helmig, D., Balsley, B., Davis, K., Kuck, L. R., Jensen, M., Bognar, J., Smith, T., Arrieta, R. V.,
628 Rodríguez, R. and Birks, J. W.: Vertical profiling and determination of landscape fluxes of
629 biogenic nonmethane hydrocarbons within the planetary boundary layer in the Peruvian Amazon,
630 *J. Geophys. Res. Atmospheres*, 103(D19), 25519–25532, doi:10.1029/98JD01023, 1998.
- 631 Helmig, D., Bocquet, F., Pollmann, J. and Revermann, T.: Analytical techniques for sesquiterpene
632 emission rate studies in vegetation enclosure experiments, *Atmos. Environ.*, 38(4), 557–572,
633 doi:10.1016/j.atmosenv.2003.10.012, 2004.
- 634 Hollesen, J., Buchwal, A., Rachlewicz, G., Hansen, B. U., Hansen, M. O., Stecher, O. and
635 Elberling, B.: Winter warming as an important co-driver for *Betula nana* growth in western
636 Greenland during the past century, in *Global change biology*, 2015.
- 637 Holst, T., Arneth, A., Hayward, S., Ekberg, A., Mastepanov, M., Jackowicz-Korczynski, M.,
638 Friberg, T., Crill, P. M. and Bäckstrand, K.: BVOC ecosystem flux measurements at a high latitude
639 wetland site, *Atmospheric Chem. Phys.*, 10(4), 1617–1634, doi:https://doi.org/10.5194/acp-10-
640 1617-2010, 2010.
- 641 Holton, J. R. and Hakim, G. J.: Chapter 8 - The Planetary Boundary Layer, in *An Introduction to*
642 *Dynamic Meteorology* (Fifth Edition), edited by J. R. Holton and G. J. Hakim, pp. 255–277,
643 Academic Press, Boston., 2013.
- 644 Honrath, R. E. and Jaffe, D. A.: The seasonal cycle of nitrogen oxides in the Arctic troposphere at
645 Barrow, Alaska, *J. Geophys. Res. Atmospheres*, 97(D18), 20615–20630, doi:10.1029/92JD02081,
646 1992.
- 647 Hu, L., Millet, D. B., Baasandorj, M., Griffis, T. J., Turner, P., Helmig, D., Curtis, A. J. and
648 Hueber, J.: Isoprene emissions and impacts over an ecological transition region in the U.S. Upper
649 Midwest inferred from tall tower measurements, *J. Geophys. Res. Atmospheres*, 120(8), 3553–
650 3571, doi:10.1002/2014JD022732, 2015.
- 651 Isaacman-VanWertz, G., Sueper, D. T., Aikin, K. C., Lerner, B. M., Gilman, J. B., de Gouw, J. A.,
652 Worsnop, D. R. and Goldstein, A. H.: Automated single-ion peak fitting as an efficient approach
653 for analyzing complex chromatographic data, *J. Chromatogr. A*, 1529, 81–92,
654 doi:10.1016/j.chroma.2017.11.005, 2017.
- 655 Jardine, K. J., Monson, R. K., Abrell, L., Saleska, S. R., Arneth, A., Jardine, A., Ishida, F. Y.,
656 Serrano, A. M. Y., Artaxo, P., Karl, T., Fares, S., Goldstein, A., Loreto, F. and Huxman, T.:
657 Within-plant isoprene oxidation confirmed by direct emissions of oxidation products methyl vinyl
658 ketone and methacrolein, *Glob. Change Biol.*, 18(3), 973–984, doi:10.1111/j.1365-
659 2486.2011.02610.x, 2012.
- 660 Kade, A., Bret-Harte, M. S., Euskirchen, E. S., Edgar, C. and Fulweber, R. A.: Upscaling of CO₂
661 fluxes from heterogeneous tundra plant communities in Arctic Alaska, *J. Geophys. Res.*
662 *Biogeosciences*, 117(G4), doi:10.1029/2012JG002065, 2012.



- 663 Karbiwnyk, C. M., Mills, C. S., Helmig, D. and Birks, J. W.: Minimization of water vapor
664 interference in the analysis of non-methane volatile organic compounds by solid adsorbent
665 sampling, *J. Chromatogr. A*, 958(1–2), 219–229, doi:10.1016/s0021-9673(02)00307-2, 2002.
- 666 Karbiwnyk, C. M., Mills, C. S., Helmig, D. and Birks, J. W.: Use of chlorofluorocarbons as internal
667 standards for the measurement of atmospheric non-methane volatile organic compounds sampled
668 onto solid adsorbent cartridges, *Environ. Sci. Technol.*, 37(5), 1002–1007,
669 doi:10.1021/es025910q, 2003.
- 670 Karl, T., Potosnak, M., Guenther, A., Clark, D., Walker, J., Herrick, J. D. and Geron, C.: Exchange
671 processes of volatile organic compounds above a tropical rain forest: Implications for modeling
672 tropospheric chemistry above dense vegetation, *J. Geophys. Res. Atmospheres*, 109(D18),
673 doi:10.1029/2004JD004738, 2004.
- 674 Kramshøj, M., Vedel-Petersen, I., Schollert, M., Rinnan, Å., Nymand, J., Ro-Poulsen, H. and
675 Rinnan, R.: Large increases in Arctic biogenic volatile emissions are a direct effect of warming,
676 *Nat. Geosci.*, 9(5), 349–352, doi:10.1038/ngeo2692, 2016.
- 677 Kulmala, M., Suni, T., Lehtinen, K. E. J., Maso, M. D., Boy, M., Reissell, A., Rannik, Ü., Aalto,
678 P., Keronen, P., Hakola, H., Bäck, J., Hoffmann, T., Vesala, T. and Hari, P.: A new feedback
679 mechanism linking forests, aerosols, and climate, *Atmospheric Chem. Phys.*, 4(2), 557–562,
680 doi:https://doi.org/10.5194/acp-4-557-2004, 2004.
- 681 Lader, R., Walsh, J. E., Bhatt, U. S. and Bieniek, P. A.: Projections of Twenty-First-Century
682 Climate Extremes for Alaska via Dynamical Downscaling and Quantile Mapping, *J. Appl.*
683 *Meteorol. Climatol.*, 56(9), 2393–2409, doi:10.1175/JAMC-D-16-0415.1, 2017.
- 684 Lappalainen, H. K., Sevanto, S., Bäck, J., Ruuskanen, T. M., Kolari, P., Taipale, R., Rinne, J.,
685 Kulmala, M. and Hari, P.: Day-time concentrations of biogenic volatile organic compounds in a
686 boreal forest canopy and their relation to environmental and biological factors, *Atmospheric*
687 *Chem. Phys.*, 9(15), 5447–5459, doi:https://doi.org/10.5194/acp-9-5447-2009, 2009.
- 688 Li, T., Holst, T., Michelsen, A. and Rinnan, R.: Amplification of plant volatile defence against
689 insect herbivory in a warming Arctic tundra, *Nat. Plants*, 5(6), 568–574, doi:10.1038/s41477-019-
690 0439-3, 2019.
- 691 Lim, H.-J., Carlton, A. G. and Turpin, B. J.: Isoprene Forms Secondary Organic Aerosol through
692 Cloud Processing: Model Simulations, *Environ. Sci. Technol.*, 39(12), 4441–4446,
693 doi:10.1021/es048039h, 2005.
- 694 Lindfors, V., Laurila, T., Hakola, H., Steinbrecher, R. and Rinne, J.: Modeling speciated terpenoid
695 emissions from the European boreal forest, *Atmos. Environ.*, 34(29), 4983–4996,
696 doi:10.1016/S1352-2310(00)00223-5, 2000.
- 697 Lindwall, F., Faubert, P. and Rinnan, R.: Diel Variation of Biogenic Volatile Organic Compound
698 Emissions- A field Study in the Sub, Low and High Arctic on the Effect of Temperature and Light,
699 *PLOS ONE*, 10(4), e0123610, doi:10.1371/journal.pone.0123610, 2015.



- 700 Lindwall, F., Schollert, M., Michelsen, A., Blok, D. and Rinnan, R.: Fourfold higher tundra volatile
701 emissions due to arctic summer warming, *J. Geophys. Res. Biogeosciences*, 121(3), 895–902,
702 doi:10.1002/2015JG003295, 2016.
- 703 Liu, X., Pawliszyn, R., Wang, L. and Pawliszyn, J.: On-site monitoring of biogenic emissions from
704 *Eucalyptus dunnii* leaves using membrane extraction with sorbent interface combined with a
705 portable gas chromatograph system, *The Analyst*, 129(1), 55–62, doi:10.1039/b311998j, 2004.
- 706 Loreto, F. and Schnitzler, J.-P.: Abiotic stresses and induced BVOCs, *Trends Plant Sci.*, 15(3),
707 154–166, doi:10.1016/j.tplants.2009.12.006, 2010.
- 708 Macias-Fauria, M., Forbes, B. C., Zetterberg, P. and Kumpula, T.: Eurasian Arctic greening
709 reveals teleconnections and the potential for structurally novel ecosystems, *Nat. Clim. Change*,
710 2(8), 613–618, doi:10.1038/nclimate1558, 2012.
- 711 Markon, C. J., Trainor, S. F. and Chapin, F. S.: The United States National Climate Assessment -
712 Alaska Technical Regional Report. [online] Available from:
713 <https://pubs.usgs.gov/circ/1379/pdf/circ1379.pdf>, 2012.
- 714 Michelsen, A., Rinnan, R. and Jonasson, S.: Two decades of experimental manipulations of heaths
715 and forest understory in the subarctic, *Ambio*, 41 Suppl 3, 218–230, doi:10.1007/s13280-012-
716 0303-4, 2012.
- 717 Millet, D. B., Alwe, H. D., Chen, X., Deventer, M. J., Griffis, T. J., Holzinger, R., Bertman, S. B.,
718 Rickly, P. S., Stevens, P. S., Léonardis, T., Locoge, N., Dusanter, S., Tyndall, G. S., Alvarez, S.
719 L., Erickson, M. H. and Flynn, J. H.: Bidirectional Ecosystem–Atmosphere Fluxes of Volatile
720 Organic Compounds Across the Mass Spectrum: How Many Matter?, *ACS Earth Space Chem.*,
721 doi:10.1021/acsearthspacechem.8b00061, 2018.
- 722 Olofsson, M., Ek-Olausson, B., Jensen, N. O., Langer, S. and Ljungström, E.: The flux of isoprene
723 from a willow coppice plantation and the effect on local air quality, *Atmos. Environ.*, 39(11),
724 2061–2070, doi:10.1016/j.atmosenv.2004.12.015, 2005.
- 725 Ortega, J. and Helmig, D.: Approaches for quantifying reactive and low-volatility biogenic organic
726 compound emissions by vegetation enclosure techniques – Part A, *Chemosphere*, 72(3), 343–364,
727 doi:10.1016/j.chemosphere.2007.11.020, 2008.
- 728 Ortega, J., Helmig, D., Daly, R. W., Tanner, D. M., Guenther, A. B. and Herrick, J. D.: Approaches
729 for quantifying reactive and low-volatility biogenic organic compound emissions by vegetation
730 enclosure techniques – Part B: Applications, *Chemosphere*, 72(3), 365–380,
731 doi:10.1016/j.chemosphere.2008.02.054, 2008.
- 732 Overland, J. E., Wang, M., Walsh, J. E. and Stroeve, J. C.: Future Arctic climate changes:
733 Adaptation and mitigation time scales, *Earths Future*, 2(2), 68–74, doi:10.1002/2013EF000162,
734 2014.
- 735 Peñuelas, J. and Staudt, M.: BVOCs and global change, *Trends Plant Sci.*, 15(3), 133–144,
736 doi:10.1016/j.tplants.2009.12.005, 2010.



- 737 Pollmann, J., Ortega, J. and Helmig, D.: Analysis of Atmospheric Sesquiterpenes: Sampling
738 Losses and Mitigation of Ozone Interferences, *Environ. Sci. Technol.*, 39(24), 9620–9629,
739 doi:10.1021/es050440w, 2005.
- 740 Potosnak, M. J., Baker, B. M., LeSturgeon, L., Disher, S. M., Griffin, K. L., Bret-Harte, M. S.
741 and Starr, G.: Isoprene emissions from a tundra ecosystem, *Biogeosciences*, 10(2), 871–889,
742 doi:10.5194/bg-10-871-2013, 2013.
- 743 Pressley, S., Lamb, B., Westberg, H., Flaherty, J., Chen, J. and Vogel, C.: Long-term isoprene flux
744 measurements above a northern hardwood forest, *J. Geophys. Res. Atmospheres*, 110(D7),
745 doi:10.1029/2004JD005523, 2005.
- 746 Reynolds, M. K., Walker, D. A., Balsler, A., Bay, C., Campbell, M., Cherosov, M. M., Daniëls, F.
747 J. A., Eidesen, P. B., Ermokhina, K. A., Frost, G. V., Jedrzejek, B., Jorgenson, M. T., Kennedy,
748 B. E., Kholod, S. S., Lavrinenko, I. A., Lavrinenko, O. V., Magnússon, B., Matveyeva, N. V.,
749 Metúsalemsson, S., Nilsen, L., Olthof, I., Pospelov, I. N., Pospelova, E. B., Pouliot, D., Razzhivin,
750 V., Schaepman-Strub, G., Šibík, J., Telyatnikov, M. Yu. and Troeva, E.: A raster version of the
751 Circumpolar Arctic Vegetation Map (CAVM), *Remote Sens. Environ.*, 232, 111297,
752 doi:10.1016/j.rse.2019.111297, 2019.
- 753 Rinnan, R., Rinnan, Å., Faubert, P., Tiiva, P., Holopainen, J. K. and Michelsen, A.: Few long-term
754 effects of simulated climate change on volatile organic compound emissions and leaf chemistry of
755 three subarctic dwarf shrubs, *Environ. Exp. Bot.*, 72(3), 377–386,
756 doi:10.1016/j.envexpbot.2010.11.006, 2011.
- 757 Rinnan, R., Steinke, M., McGenity, T. and Loreto, F.: Plant volatiles in extreme terrestrial and
758 marine environments, *Plant Cell Environ.*, 37(8), 1776–1789, doi:10.1111/pce.12320, 2014.
- 759 Rinne, H. J. I., Guenther, A. B., Greenberg, J. P. and Harley, P. C.: Isoprene and monoterpene
760 fluxes measured above Amazonian rainforest and their dependence on light and temperature,
761 *Atmos. Environ.*, 36(14), 2421–2426, doi:10.1016/S1352-2310(01)00523-4, 2002.
- 762 Rinne, J., Bäck, J. and Hakola, H.: Biogenic volatile organic compound emissions from the
763 Eurasian taiga: current knowledge and future directions, , 14, 20, 2009.
- 764 Rivera-Rios, J. C., Nguyen, T. B., Crouse, J. D., Jud, W., Clair, J. M. S., Mikoviny, T., Gilman,
765 J. B., Lerner, B. M., Kaiser, J. B., Gouw, J. de, Wisthaler, A., Hansel, A., Wennberg, P. O.,
766 Seinfeld, J. H. and Keutsch, F. N.: Conversion of hydroperoxides to carbonyls in field and
767 laboratory instrumentation: Observational bias in diagnosing pristine versus anthropogenically
768 controlled atmospheric chemistry, *Geophys. Res. Lett.*, 41(23), 8645–8651,
769 doi:10.1002/2014GL061919, 2014.
- 770 Ruuskanen, T. M., Kolari, P., Bäck, J., Kulmala, M., Rinne, J., Hakola, H., Taipale, R., Raivonen,
771 M., Altimir, N. and Hari, P.: On-line field measurements of monoterpene emissions from Scots
772 pine by proton-transfer-reaction mass spectrometry, *Boreal Environ. Res.*, 10(6), 553–567, 2005.



- 773 Scanlon, J. T. and Willis, D. E.: Calculation of Flame Ionization Detector Relative Response
774 Factors Using the Effective Carbon Number Concept, *J. Chromatogr. Sci.*, 23(8), 333–340,
775 doi:10.1093/chromsci/23.8.333, 1985.
- 776 Schollert, M., Burchard, S., Faubert, P., Michelsen, A. and Rinnan, R.: Biogenic volatile organic
777 compound emissions in four vegetation types in high arctic Greenland, *Polar Biol.*, 37(2), 237–
778 249, doi:10.1007/s00300-013-1427-0, 2014.
- 779 Shaver, G. R. and Chapin, F. S.: Production: Biomass Relationships and Element Cycling in
780 Contrasting Arctic Vegetation Types, *Ecol. Monogr.*, 61(1), 1–31, doi:10.2307/1942997, 1991.
- 781 Sindelarova, K., Granier, C., Bouarar, I., Guenther, A., Tilmes, S., Stavrakou, T., Müller, J.-F.,
782 Kuhn, U., Stefani, P. and Knorr, W.: Global data set of biogenic VOC emissions calculated by the
783 MEGAN model over the last 30 years, *Atmospheric Chem. Phys.*, 14(17), 9317–9341,
784 doi:https://doi.org/10.5194/acp-14-9317-2014, 2014.
- 785 Sistla, S. A., Moore, J. C., Simpson, R. T., Gough, L., Shaver, G. R. and Schimel, J. P.: Long-term
786 warming restructures Arctic tundra without changing net soil carbon storage, *Nature*, 497(7451),
787 615–618, doi:10.1038/nature12129, 2013.
- 788 Spirig, C., Guenther, A., Greenberg, J. P., Calanca, P. and Tarvainen, V.: Tethered balloon
789 measurements of biogenic volatile organic compounds at a Boreal forest site, *Atmospheric Chem.*
790 *Phys.*, 4(1), 215–229, doi:https://doi.org/10.5194/acp-4-215-2004, 2004.
- 791 Sturm, M., Racine, C. and Tape, K.: Increasing shrub abundance in the Arctic, *Nature*, 411(6837),
792 546–547, doi:10.1038/35079180, 2001.
- 793 Sullivan, P. F., Sommerkorn, M., Rueth, H. M., Nadelhoffer, K. J., Shaver, G. R. and Welker, J.
794 M.: Climate and species affect fine root production with long-term fertilization in acidic tussock
795 tundra near Toolik Lake, Alaska, *Oecologia*, 153(3), 643–652, doi:10.1007/s00442-007-0753-8,
796 2007.
- 797 Survey: Maps - Toolik Lake Area Vegetation, [online] Available from:
798 <http://www.arcticatlas.org/maps/themes/tl5k/tl5kvg> (Accessed 30 September 2019), 2012.
- 799 Tang, J., Schurgers, G., Valolahti, H., Faubert, P., Tiiva, P., Michelsen, A. and Rinnan, R.:
800 Challenges in modelling isoprene and monoterpene emission dynamics of Arctic plants: a case
801 study from a subarctic tundra heath, *Biogeosciences*, 13(24), 6651–6667,
802 doi:https://doi.org/10.5194/bg-13-6651-2016, 2016.
- 803 Tape, K., Sturm, M. and Racine, C.: The evidence for shrub expansion in Northern Alaska and the
804 Pan-Arctic, *Glob. Change Biol.*, 12(4), 686–702, doi:10.1111/j.1365-2486.2006.01128.x, 2006.
- 805 Tarvainen, V., Hakola, H., Rinne, J., HellåN, H. and Haapanala, S.: Towards a comprehensive
806 emission inventory of terpenoids from boreal ecosystems, *Tellus B Chem. Phys. Meteorol.*, 59(3),
807 526–534, doi:10.1111/j.1600-0889.2007.00263a.x, 2007.



- 808 Tiiva, P., Faubert, P., Michelsen, A., Holopainen, T., Holopainen, J. K. and Rinnan, R.: Climatic
809 warming increases isoprene emission from a subarctic heath, *New Phytol.*, 180(4), 853–863,
810 doi:10.1111/j.1469-8137.2008.02587.x, 2008.
- 811 Toolik Field Station Environmental Data Center: Toolik Field Station::Weather Data Query,
812 [online] Available from: https://toolik.alaska.edu/edc/abiotic_monitoring/data_query.php
813 (Accessed 30 September 2019), 2019.
- 814 Tsigaridis, K. and Kanakidou, M.: Secondary organic aerosol importance in the future atmosphere,
815 *Atmos. Environ.*, 41(22), 4682–4692, doi:10.1016/j.atmosenv.2007.03.045, 2007.
- 816 Unger, N.: Human land-use-driven reduction of forest volatiles cools global climate, *Nat. Clim.*
817 *Change*, 4(10), 907–910, doi:10.1038/nclimate2347, 2014.
- 818 Valolahti, H., Kivimäenpää, M., Faubert, P., Michelsen, A. and Rinnan, R.: Climate change-
819 induced vegetation change as a driver of increased subarctic biogenic volatile organic compound
820 emissions, *Glob. Change Biol.*, 21(9), 3478–3488, doi:10.1111/gcb.12953, 2015.
- 821 Van Dam, B., Helmig, D., Burkhardt, J. F., Obrist, D. and Oltmans, S. J.: Springtime boundary layer
822 O₃ and GEM depletion at Toolik Lake, Alaska, *J. Geophys. Res. Atmospheres*, 118(8), 3382–
823 3391, doi:10.1002/jgrd.50213, 2013.
- 824 Vedel-Petersen, I., Schollert, M., Nymand, J. and Rinnan, R.: Volatile organic compound emission
825 profiles of four common arctic plants, *Atmos. Environ.*, 120, 117–126,
826 doi:10.1016/j.atmosenv.2015.08.082, 2015.
- 827 Walker, M. D., Walker, D. A. and Auerbach, N. A.: Plant communities of a tussock tundra
828 landscape in the Brooks Range Foothills, Alaska, *J. Veg. Sci.*, 5(6), 843–866,
829 doi:10.2307/3236198, 1994.
- 830 Wang, J.-L., Chew, C., Chen, S.-W. and Kuo, S.-R.: Concentration Variability of Anthropogenic
831 Halocarbons and Applications as Internal Reference in Volatile Organic Compound
832 Measurements, *Environ. Sci. Technol.*, 34(11), 2243–2248, doi:10.1021/es991128n, 2000.
- 833 Zini, C. A., Augusto, F., Christensen, T. E., Smith, B. P., Caramão, E. B. and Pawliszy, J.:
834 Monitoring biogenic volatile compounds emitted by *Eucalyptus citriodora* using SPME, *Anal.*
835 *Chem.*, 73(19), 4729–4735, doi:10.1021/ac0103219, 2001.
- 836



837 Table 1: Year 2017 median relative percent cover of plant species in moist acidic tundra long-term
 838 ecological research (LTER) experimental control plots at Toolik Field Station. The last column
 839 indicates whether plant species were present in surface or bag enclosure experiments in this study.

Plant name	Relative land surface cover in moist acidic tundra (%) (Gough, 2019)	Present in surface or bag enclosures
<i>Andromeda polifolia</i>	0.6	yes
<i>Betula nana</i>	14.4	yes
<i>Carex bigelowii</i>	1.0	yes
<i>Cassiope tetragona</i>	2.0	yes
<i>Empetrum nigrum</i>	3.8	yes
<i>Eriophorum vaginatum</i>	8.6	yes
<i>Ledum palustre</i>	10.5	yes
<i>Mixed Lichens</i>	2.1	yes
<i>Mixed moss</i>	6.0	yes
<i>Pedicularis lapponica</i>	0.6	no
<i>Polygonum bistorta</i>	0.6	no
<i>Rubus chamaemorus</i>	20.2	no
<i>Salix pulchra</i>	4.9	yes
<i>Vaccinium uliginosum</i>	1.9	yes
<i>Vaccinium vitis-idaea</i>	6.6	yes

840

841

842

843

844



845 Table 2: Average mixings ratios with standard deviation, along with minimum (min) and
846 maximum (max) values and quantification frequency (QF) of the measured monoterpenes in
847 ambient air. LOQ stands for limit of quantification. For values lower than the LOQ, mixing ratios
848 equal to half of the LOQ were used to calculate the mean.

	mean \pm standard deviation (pptv)	Min (pptv)	Max (pptv)	QF (%)
α -pinene	11.7 \pm 8.1	< LOQ	61.6	88
camphene	< LOQ	< LOQ	21.9	11
sabinene	< LOQ	< LOQ	34.2	11
p-cymene	2.0 \pm 1.9	< LOQ	12.3	32
limonene	< LOQ	< LOQ	2.9	< 1

849

850

851

852

853

854

855

856

857

858

859

860

861

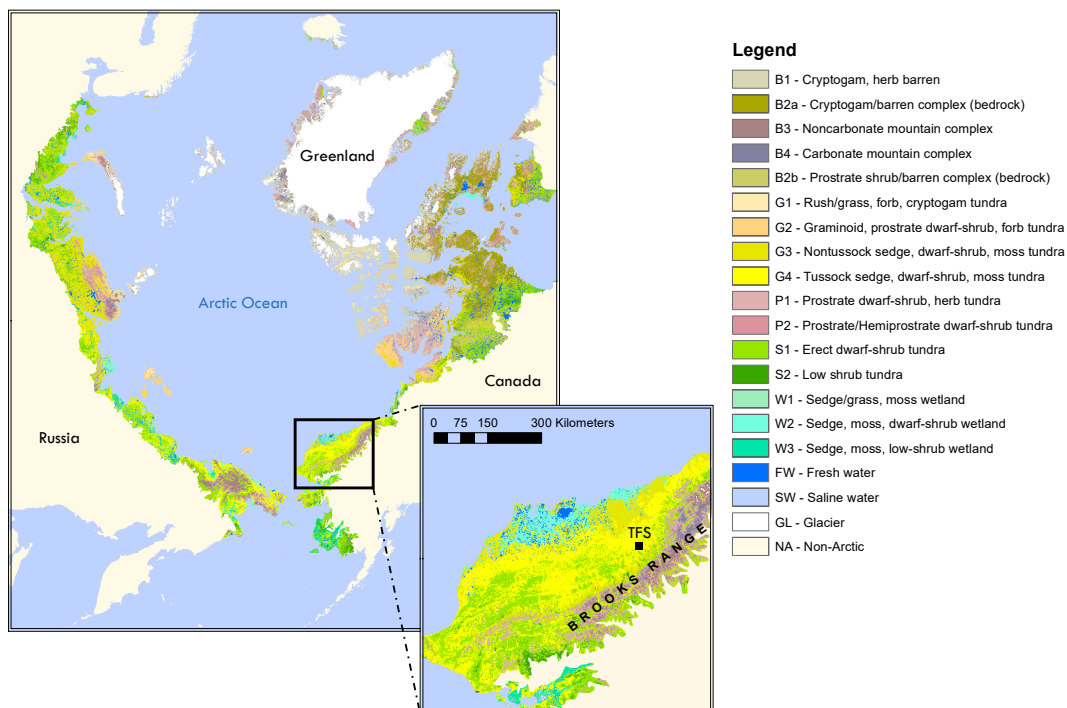
862



863 Table 3: Isoprene and monoterpenes (sum of α -pinene, β -pinene, limonene, and 1,8-cineole) surface
 864 emission rates per vegetation type. Miscellaneous refers to a mix of different species, including lichens
 865 and moss tundra (see Fig.S.I.3-15). Daytime refers to 10 am-8 pm, midday to 11 am-2 pm, and nighttime
 866 to 11 pm-5 am (Alaska Standard Time).

	mean \pm standard deviation ($\mu\text{gC}/\text{m}^2/\text{h}$)	daytime mean \pm standard deviation ($\mu\text{gC}/\text{m}^2/\text{h}$)	midday mean \pm standard deviation ($\mu\text{gC}/\text{m}^2/\text{h}$)	nighttime mean \pm standard deviation ($\mu\text{gC}/\text{m}^2/\text{h}$)
isoprene				
<i>Salix</i> spp.	149 \pm 327	232 \pm 400	334 \pm 473	7 \pm 10
<i>Betula</i> spp.	12 \pm 30	19 \pm 38	28 \pm 37	5 \pm 14
Miscellaneous	38 \pm 81	57 \pm 100	104 \pm 135	21 \pm 64
monoterpenes				
<i>Salix</i> spp.	0.8 \pm 1.3	1.1 \pm 1.5	1.4 \pm 1.7	0.4 \pm 1.0
<i>Betula</i> spp.	0.5 \pm 0.6	0.7 \pm 0.7	1.0 \pm 0.8	0.2 \pm 0.2
Miscellaneous	1.1 \pm 1.4	1.3 \pm 1.6	1.7 \pm 2.0	1.0 \pm 1.4

867
 868
 869
 870
 871
 872
 873
 874
 875



876

877 Figure 1: Location of Toolik Field Station (TFS) on the north flanks of the Brooks Range in northern Alaska
878 along with arctic vegetation type. This Figure was made using the raster version of the Circumpolar Arctic
879 Vegetation Map prepared by Reynolds et al. (2019) and publicly available at www.geobotany.uaf.edu.

880

881

882

883

884

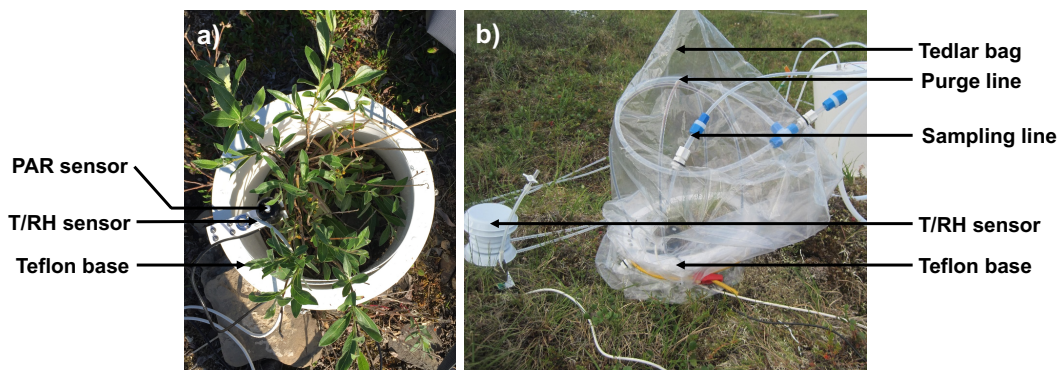
885

886

887

888

889



890

891 Figure 2: Photographs of a surface enclosure experiment setup at Toolik Field Station, Alaska. a) The first
892 step of the installation consisted in positioning the Teflon® base around the vegetation of interest along
893 with temperature (T), relative humidity (RH), and photosynthetically active radiation (PAR) sensors. b)
894 The second step consisted in positioning the Tedlar® bag around the base. The bag was connected to a
895 purge air and a sampling line. An additional T/RH sensor was also positioned outside the bag.

896

897

898

899

900

901

902

903

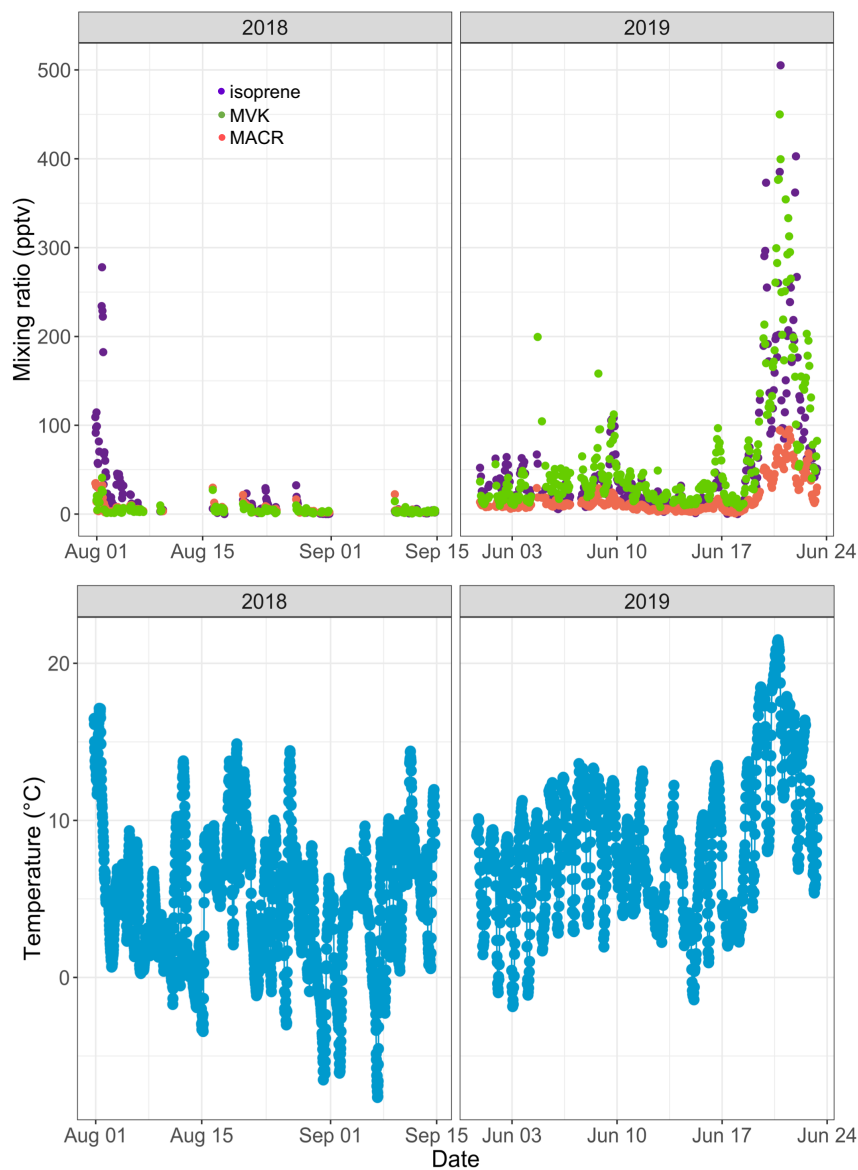
904

905

906

907

908

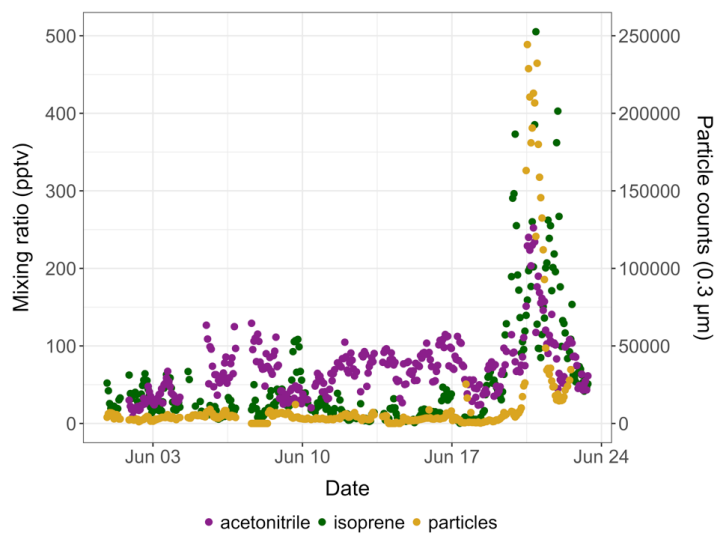


909

910 Figure 3: Time-series of isoprene (purple), methylvinylketone (MVK, green), and methacrolein (MACR,
911 salmon) mixing ratios (in pptv) in ambient air at Toolik Field station (top panels) and of 30-min-averaged
912 ambient temperature (in °C) at 4 meters above ground level (bottom panels).

913

914



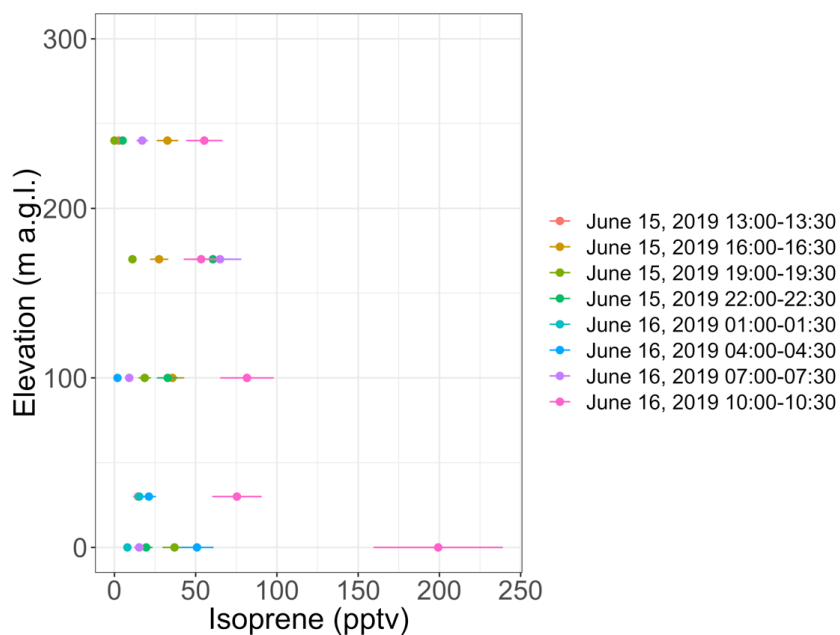
915

916 Figure 4: Time-series of isoprene (green) and acetonitrile (purple) mixing ratios (in pptv) and of 0.3 μm
917 particle counts (yellow) in ambient air at Toolik Field station in June 2019.

918

919

920



921

922 Figure 5: Vertical profile of isoprene mixing ratios as inferred from 30-min samples collected with a
923 tethered balloon. The error bars show the analytical uncertainty for isoprene (20 %). Samples with an
924 isoprene mixing ratio lower than blanks were discarded. Hours are in Alaska Standard Time (UTC-9).

925

926

927

928

929

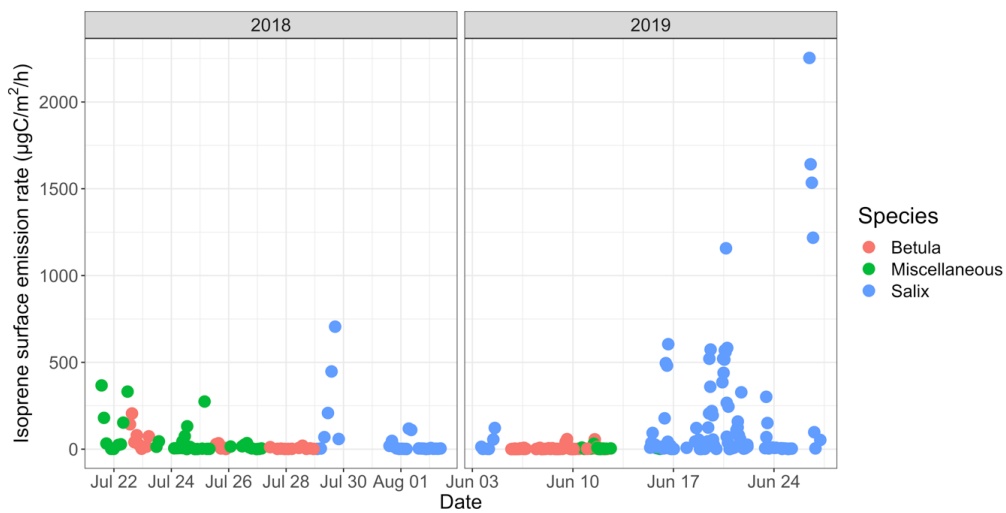
930

931

932

933

934



935

936 Figure 6: Time-series of isoprene surface emission rates (in $\mu\text{gC}/\text{m}^2/\text{h}$) for different vegetation types.

937

938

939

940

941

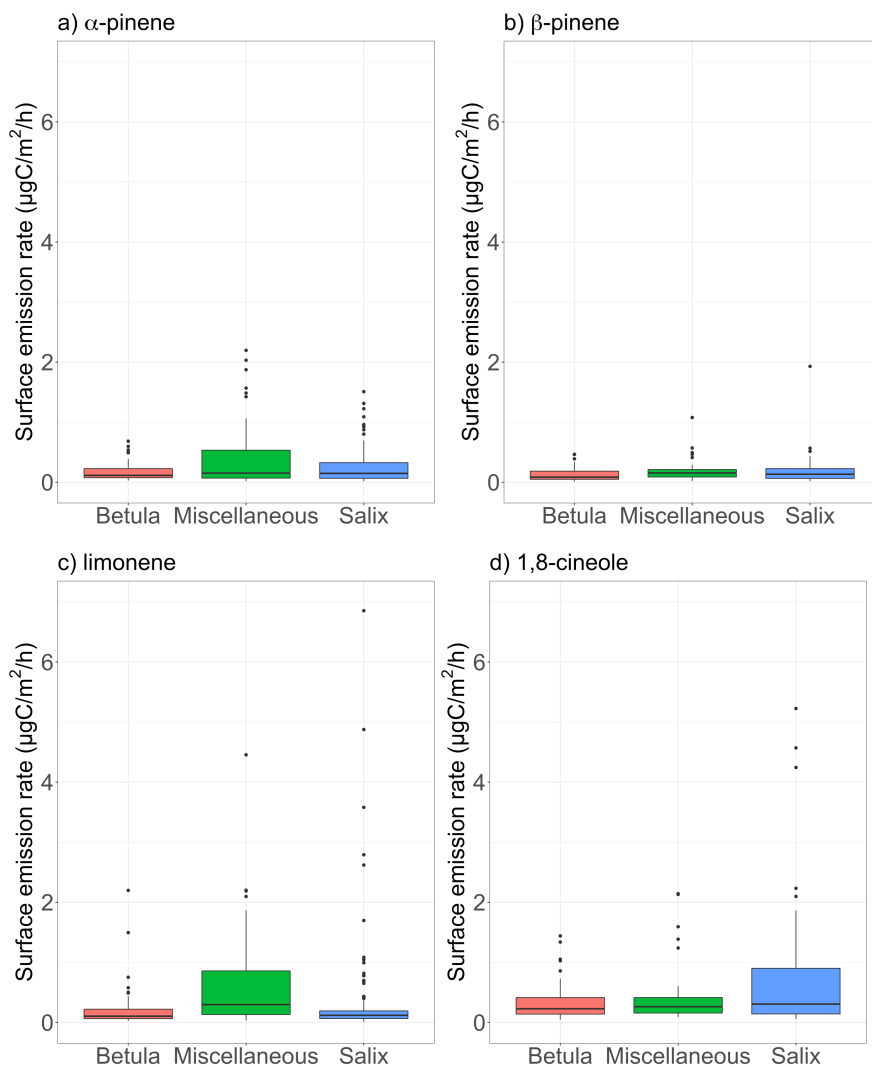
942

943

944

945

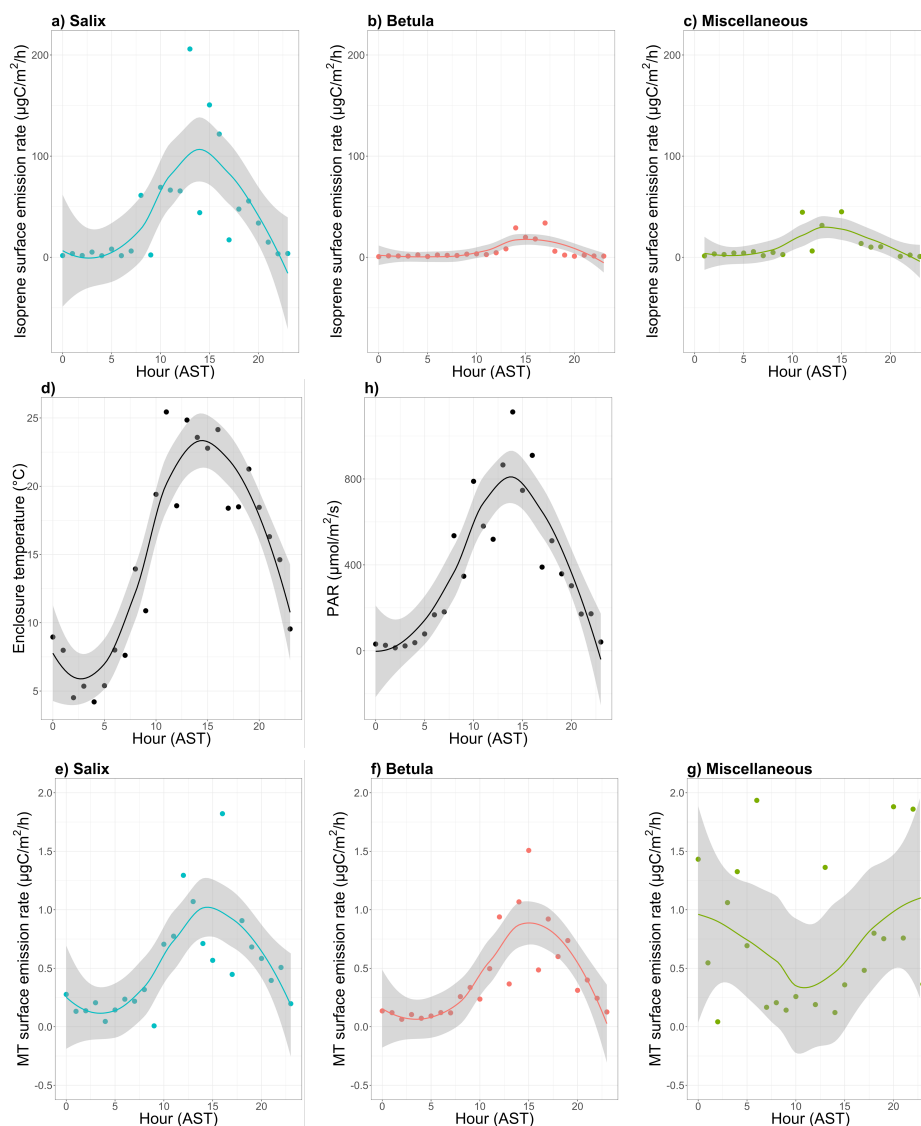
946



947

948 Figure 7: Surface emission rates of various monoterpenes (in $\mu\text{gC}/\text{m}^2/\text{h}$) for different vegetation types. The
949 lower and upper hinges correspond to the first and third quartiles. The upper (lower) whisker extends from
950 the hinge to the largest (smallest) value no further than $1.5 \times IQR$ from the hinge, where IQR is the inter-
951 quartile range (i.e., the distance between the first and third quartiles). The notches extend $1.58 \times IQR/\sqrt{n}$
952 and give a $\sim 95\%$ confidence interval for medians.

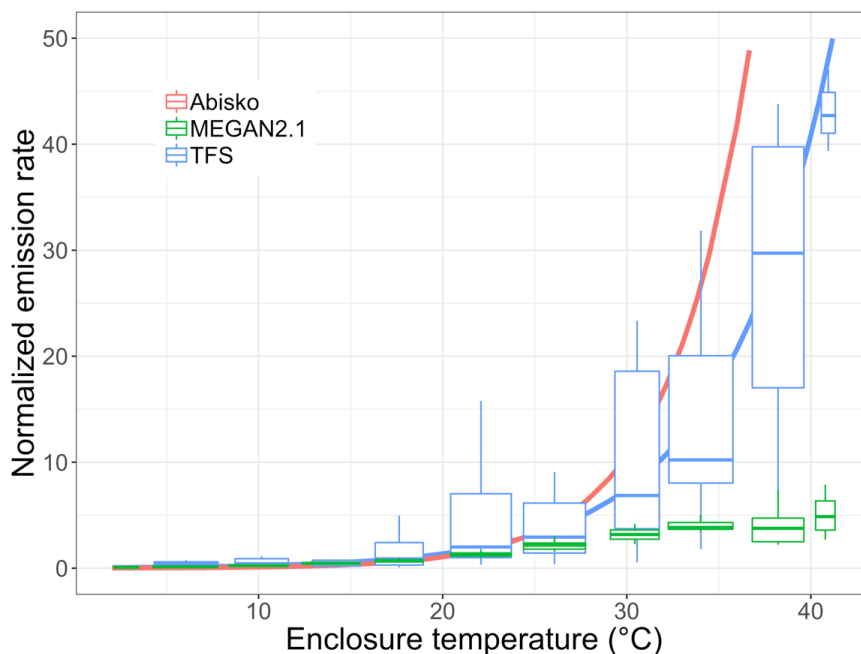
953



954

955 Figure 8: Mean diurnal cycle of isoprene (a-c) and monoterpenes (MT; e-g) surface emission rates (in
956 $\mu\text{gC}/\text{m}^2/\text{h}$ – note the difference scale on the y-axis), d) enclosure temperature (in $^{\circ}\text{C}$), and h) enclosure
957 photosynthetically active radiation (PAR in $\mu\text{mol}/\text{m}^2/\text{s}$). The dots represent the hourly means. The line is
958 the smoothed conditional mean while the grey shaded region indicates the 95% confidence interval. Hours
959 are in Alaska Standard Time (UTC-9) and correspond to the end of the 2-hr sampling period for isoprene
960 and MT emission rates. MT corresponds here to the sum of α -pinene, β -pinene, limonene, and 1,8-cineole.

961



962

963 Figure 9: Normalized isoprene surface emission rate (emissions at 20°C set equal to 1.0) as a function of
964 enclosure temperature (in °C). This figure shows the response to temperature as observed at Toolik Field
965 Station (TFS, in blue) and Abisko, Sweden (in pink; Tang et al., 2016), and as parameterized in MEGAN2.1
966 (in green). The blue solid line is the exponential fit at TFS. It should be noted that the enclosure temperature
967 was on average 5-6°C warmer than ambient air due to greenhouse heating.